# Two-state swimming: Strategy and survival of a model bacterial predator in response to environmental cues

Lance W. Q. Xu (徐伟青),[1,2] J. Shepard Bryan IV,[1,2] Zeliha Kilic,[3] and Steve Pressé[1,2,4,*]

[1]Department of Physics, Arizona State University, Tempe, Arizona; [2]Center for Biological Physics, Arizona State University, Tempe, Arizona; [3]Single-Molecule Imaging Center, Saint Jude's Children Hospital, Memphis, Tennessee; and [4]School of Molecular Sciences, Arizona State University, Tempe, Arizona

ABSTRACT *Bdellovibrio bacteriovorus* is a predatory bacterium preying upon Gram-negative bacteria. As such, *B. bacteriovorus* has the potential to control antibiotic-resistant pathogens and biofilm populations. To survive and reproduce, *B. bacteriovorus* must locate and infect a host cell. However, in the temporary absence of prey, it is largely unknown how *B. bacteriovorus* modulate their motility patterns in response to physical or chemical environmental cues to optimize their energy expenditure. To investigate *B. bacteriovorus*' predation strategy, we track and quantify their motion by measuring speed distributions as a function of starvation time. While an initial unimodal speed distribution relaxing to one for pure diffusion at long times may be expected, instead we observe a bimodal speed distribution with one mode centered around that expected from diffusion and the other centered at higher speeds. What is more, for an increasing amount of time over which *B. bacteriovorus* is starved, we observe a progressive reweighting from the active swimming state to an apparent diffusive state in the speed distribution. Distributions of trajectory-averaged speeds for *B. bacteriovorus* are largely unimodal, indicating switching between a faster swim speed and an apparent diffusive state within individual observed trajectories rather than there being distinct active swimming and apparent diffusive populations. We also find that *B. bacteriovorus*' apparent diffusive state is not merely caused by the diffusion of inviable bacteria as subsequent spiking experiments show that bacteria can be resuscitated and bimodality restored. Indeed, starved *B. bacteriovorus* may modulate the frequency and duration of active swimming as a means of balancing energy consumption and procurement. Our results thus point to a reweighting of the swimming frequency on a trajectory basis rather than a population level basis.

SIGNIFICANCE *Bdellovibrio bacteriovorus* is a predatory bacterium that may help control Gram-negative bacterial populations in environmental and clinical settings. To locate its prey in solution, *B. bacteriovorus* must expend energy to fight hydrodynamic drag. This raises the question as to how *B. bacteriovorus* should expend its energy reserves in the absence of chemical cues from its prey. Here, we show that *B. bacteriovorus* adapts its motility to minimize energy expenditure (due to fighting drag in swimming) upon prolonged starvation by exploiting two motility states.

## INTRODUCTION

Bacterial cues drawn from the environment—mediated through a number of factors such as hydrodynamic interactions (1,2), external flows (3–5), or other direct chemical signaling and quorum sensing (6–12)—are critical in understanding cell-cell interaction and emergent collective behaviors of biomedical interest (7,13,14) such as biofilm formation (15) and bacterial swarming (16,17).

Here, our focus is in understanding the hunting strategy of predatory bacteria, such as *Bdellovibrio* and like organisms (sometimes called BALOs), driven by external resources. Understanding such strategies is helpful in exploiting *Bdellovibrio* and like organisms for a number of tasks including the degradation of hazardous microbial biofilms on surfaces (15,18–21), purifying water and soil (22–24), and serving as a "living antibiotic" (14,25,26) by reducing pulmonary bacterial infections in rats (27), gut infections in poultry (28), corneal infections in rabbits (29), and infections in other

animal models such as zebrafish (30). Indeed, the bacterial predator, *Bdellovibrio bacteriovorus*, has been shown to significantly decrease populations of many other species of Gram-negative bacteria (31,32) across habitats (14,15,18,19,22–24,28–30,33,34).

The biphasic life cycle of *B. bacteriovorus* involves an attack phase in which predatory *B. bacteriovorus* locate their bacterial prey and enter the periplasm where they complete the replicative growth phase, ending with the progeny lysing from the host (35–41). Although *B. bacteriovorus* was discovered half a century ago (42–44) and is now studied as a model predator, it is largely unknown how *B. bacteriovorus* locate individual prey. For instance, previous studies suggested that *B. bacteriovorus* bumps into its prey at random (19,22,34,38,45–48).

In previous work, we revisited this hypothesis (2) and investigated the role hydrodynamics plays in *B. bacteriovorus*' hunting strategy. Our own previous efforts built upon recent literature suggesting that bacteria sense and respond to environmental hydrodynamic flows (3–5) and self-generated flows (1,49–54). In particular, we found that, on account of *B. bacteriovorus*' unusually high speed, passive hydrodynamic forces could drive it toward surfaces where prey tend to be present in larger numbers (2), thereby improving the odds of a chance collision.

This finding raises the following question: given that hydrodynamic forces induced by *B. bacteriovorus*' unusually high speeds are critical in bringing it toward prey, how might *B. bacteriovorus*, in the absence of prey in its environment, allocate its energy reserves to overcome hydrodynamic drag as it propels itself through solution in search of prey? Naively, one may expect a unimodal speed distribution at high speeds across a trajectory to shift to a unimodal speed distribution at longer times to coincide with a peak around that expected for pure diffusion. On the other hand, prey bacteria such as *E. coli* are known to modulate swimming behavior based on environmental cues (55,56) (mainly the presence of predator bacteria) so it does not seem unreasonable to expect the predator to modulate its swimming behavior in the presence of prey.

A naive search strategy where active motility persists until the available energy—used to maintain metabolic homeostasis, as well as overcoming both translational and rotational hydrodynamic drag—is expended may suggest that *B. bacteriovorus* would not be revivable once energy resources are depleted and, possibly, that its proteome might be catabolized in an effort to locate prey by active swimming. On the other hand, an alternative use of energy may involve the active modulation of motility as a function of both internal energy reserves (i.e., age) and environmental cues (i.e., potential sources of energy and nutrients) before reaching a point of no return, at which point *B. bacteriovorus* would no longer have the reserves needed to fight hydrodynamic drag in search of prey despite external cues suggesting its availability. We partly address

this question by monitoring changes in large numbers of *B. bacteriovorus* trajectories under starvation conditions as a function of age and buffer conditions. We found that key dynamical features—instantaneous and trajectory-averaged speed distributions—monitored over the course of 40 h may suggest behavior consistent with what can described as an exploitative search strategy.

We corroborated these results by subsequently performing spiking experiments in which starved bacteria are resuspended in rich media, showing that *B. bacteriovorus* can be resuscitated and their active motility restored. Our results help shed light on the compromises *B. bacteriovorus* must make when hunting in the absence of environmental cues and how switching between an active state and an apparent diffusive state can be used to cope with unfavorable environmental conditions.

## MATERIALS AND METHODS

### Bacterial strains and growth conditions

To avoid any possible variations in the motile behavior of *B. bacteriovorus* due to expression of a fluorescent protein, the wild-type strain 109 (Bdellovibrio bacteriovorus Stolp and Starr, ATTC no. 15143; American Type Culture Collection, Manassas, VA) was used to carry out these studies. *Escherichia coli* strain OP50 which was grown in lysogeny broth (LB) (10 g/L yeast extract, 20 g/L tryptone, 20 g/L sodium chloride [pH 7.5]) at 37°C on a 300-rpm shaker was used as *B. bacteriovorus*' prey. After multiple washes with HEPES medium, the OD (600 nm) was taken of the *E. coli* and the bacteria were stored at 4°C until use for synchronization cultures as described below.

### Synchronization of *B. bacteriovorus*

Modifications to the synchronization protocols outlined in the literature (7,57) allow for the synchronized observation of many *B. bacteriovorus* of the same age. This was achieved by growing *B. bacteriovorus* in nutrient-poor medium (HEPES medium [HM]) (25 mM HEPES [pH 7.4], 3 mM $CaCl_2$, 2 mM $MgCl_2$) containing approximately $10^8$ (OD 1) *E. coli* cells overnight at 28°C on a 300-rpm shaker. The next day, *B. bacteriovorus* was isolated by centrifugation at 7900 rpm for 30 min at 4°C. The predators were then resuspended in fresh HM buffer containing *E. coli* cells at 0.7 OD. An hour after introduction to fresh *E. coli*, the formed bdelloplasts were isolated and resuspended in fresh medium several times via centrifugation (2000 rpm for 10 min at room temperature). This eliminated the majority of leftover predators. After an additional 4 h, the lysed progeny were collected by passing the culture through a 0.45-$\mu$m Millex HP syringe filter twice. The isolated *B. bacteriovorus* remained in nutrient-poor medium to begin starvation conditions.

The effectiveness of the isolation method was tested by passing an *E. coli* OP50 culture of OD 1 through the filter and adding nutrient-rich medium. The culture was monitored for several days, with no bacteria growing, showing that *E. coli* was effectively removed by filtration.

### Starvation of *B. bacteriovorus* experiments

The synchronized *B. bacteriovorus* was obtained as described above. The culture remained shaking at 28°C on a 300-rpm shaker during the total duration of the experiment (approximately 48 h). A small aliquot was taken from the culture every hour for sample preparation and data acquisition described below.

## Spiking of *B. bacteriovorus* with rich medium experiments

The *B. bacteriovorus* was synchronized as described above. Four hours after the culture was filtered, the culture was divided into three 2-mL total volumes: a control, and two cultures that were spiked with rich medium. The *B. bacteriovorus* was spiked with nutrient-rich medium, LB (10 g/L yeast extract, 20 g/L tryptone, 20 g/L NaCl [pH 7.5]) at hour 4 and hour 20 after filtration. The cultures that were spiked had 1.75 mL of *B. bacteriovorus* added and 0.25 mL of rich medium. The cultures remained shaking at 28°C on a 300-rpm shaker during the total duration of the experiment. Small aliquots were taken from the three cultures for measurements.

## Memory of *B. bacteriovorus* experiments

The *B. bacteriovorus* was synchronized according to synchronization of *B. bacteriovorus*. Six hours after filtration, the culture was divided into three 2-mL total volumes: a control, and two cultures that were spiked with rich medium at hour 6. The cultures that were spiked had 1.75 mL of *B. bacteriovorus* added and 0.25 mL of rich medium. The cultures were observed 15 min after exposure. To initiate starvation conditions again, all three cultures were centrifuged (30 min after initial exposure time) at 13,000 rpm for 4 min at room temperature. The control culture and one of the spiked cultures were resuspended in 2 mL fresh HM. The other spiked culture was resuspended in 1.75 mL of HM and 0.25 mL of LB. (58). The cultures remained shaking at 28°C on a 300-rpm shaker during the total duration of the experiment. Small aliquots were taken from the three cultures for measurements. The effects of centrifugation can be seen in Fig. S2.

## Sample preparation

A small volume (10 $\mu$L) of the culture was aliquoted onto a microscope coverslip containing vacuum grease along the outer edge and secured with a slide. Focusing on the midplane (approximately 70 $\mu$m from the surface) allowed for the observation of the bacteria without restricting their movement due to a confined vertical depth (2).

## Data acquisition

Using an inverted phase contrast microscope (Nikon, Melville, NY), the bacteria were imaged with a 1024 × 1024 pixel ROI using a 60× (1.4 NA) oil immersion objective. Each hour data were collected by recording six 20-s videos at 8 ms exposure using a Hamamatsu (Shizuoka, Japan) ORCA-Flash4.0 3V sCMOS camera. These videos were then processed to obtain velocity distributions over thousands of bacterial trajectories as described in data analysis.

## Data analysis

The bacteria in the images are clearly visible by eye and could in principle be tracked by hand (Fig. S3). However, due to the volume of data, we automated tracking. The motility of the bacteria was tracked by using a package for feature detection, TrackPy (59), which provides the ability to locate features (e.g., bacteria) in raw image data and link those features across frames into trajectories. Two of the main parameters used for locating features were the diameter and minmass. The diameter is determined based on the size of the object tracked and the minmass is the minimum integrated brightness used to eliminate spurious features. As *B. bacteriovorus* is about 1 $\mu$m long (i.e., 11 pixels), we conservatively chose an all-inclusive 15-pixel diameter. The minmass varies between runs given the overall brightness of the video. Changes in this value may affect the overall number of bacteria tracked within the focal plane, but would not influence conclusions drawn on the overall motility of individual bacteria; i.e., it only reduces the statistics available. To link bacteria across frames, the search range was consistently set to 20 pixels as the bacteria are unlikely to travel further than this number of pixels between consecutive frames (19). As bacteria move in and out of focus, there is a sampling bias in speed measurements at the start and end of trajectories toward slow speeds (i.e., a bias toward a larger velocity component *orthogonal* to the focal plane). Removing the first and last two frames of all trajectories was sufficient to mitigate this bias (Fig. S4; Table S1). Also for this reason, we ignored any traces shorter than 10 consecutive frames.

Window averaging of the bacterium's position was calculated to more accurately track its movement. The effect of different windows can be seen in Fig. S5. Based on these results, a window of three was used for all bacteria located. As windowing essentially decreases the number of original data points, we also tested downsampling (decimating) the data to assure ourselves that the shape of the distributions did not greatly vary (Fig. S6).

Once each trajectory is recorded as a time series of two-dimensional coordinates, the distance the feature moves between each consecutive frame and the exposure time of the camera are used to calculate the instantaneous speeds. A central difference of the positions with respect to time was used to get a more accurate speed estimate. The average speed for each trajectory was obtained by taking the average of the instantaneous speeds of each bacterium's trajectory along the whole trajectory.

For robustness, we compared the above tracking method with a method leveraging neural networks to localize the bacteria, and parameter-free Gaussian process regression to obtain velocities at each frame (see supporting material). In brief, key results uncovered in the speed histograms (namely bimodality, discussed shortly) (Figs. 1 and 2), were recovered using the parameter-free analysis, further suggesting that the bimodality is a feature of the data and not a tracking artifact.

## RESULTS

To see how *B. bacteriovorus* adapts to environmental cues, we first observed the swimming behavior of synchronized *B. bacteriovorus* in the absence of prey and nutrients. The bacterial trajectories after different periods of starvation can be seen in Fig. 3, in which the normalized speeds are plotted in blue. Under such starvation conditions, we monitored the instantaneous speed of each bacterium at each frame as well as the average speed of each bacterium along its trajectory (Fig. 1). The instantaneous speed is obtained using the smoothing algorithm described in the materials and methods. The average speed of each bacterium is simply the average of the instantaneous speeds for the bacterium. We uncover a reproducible bimodal instantaneous speed distribution with peaks at roughly 10 and 40 $\mu$m s$^{-1}$ with the relative weight of each peak being sensitive to *B. bacteriovorus*' age and buffer conditions.

We then introduced *B. bacteriovorus* to nutrient-rich medium (LB)—effectively providing them with an external energy source—to determine whether the bacteria were merely inviable or swimming less frequently at later times. We monitored the changes in the speed distributions (Fig. 2) compared with a starving control of equal age.

To further investigate the nature of *B. bacteriovorus*' search strategy bimodal speed distribution, we monitored *B. bacteriovorus*' behavior with a cycle of starvation, rich medium exposure, and then restarvation. This resulted in bacteria repopulating the active swimming state and then the apparent diffusive state (Fig. S7).
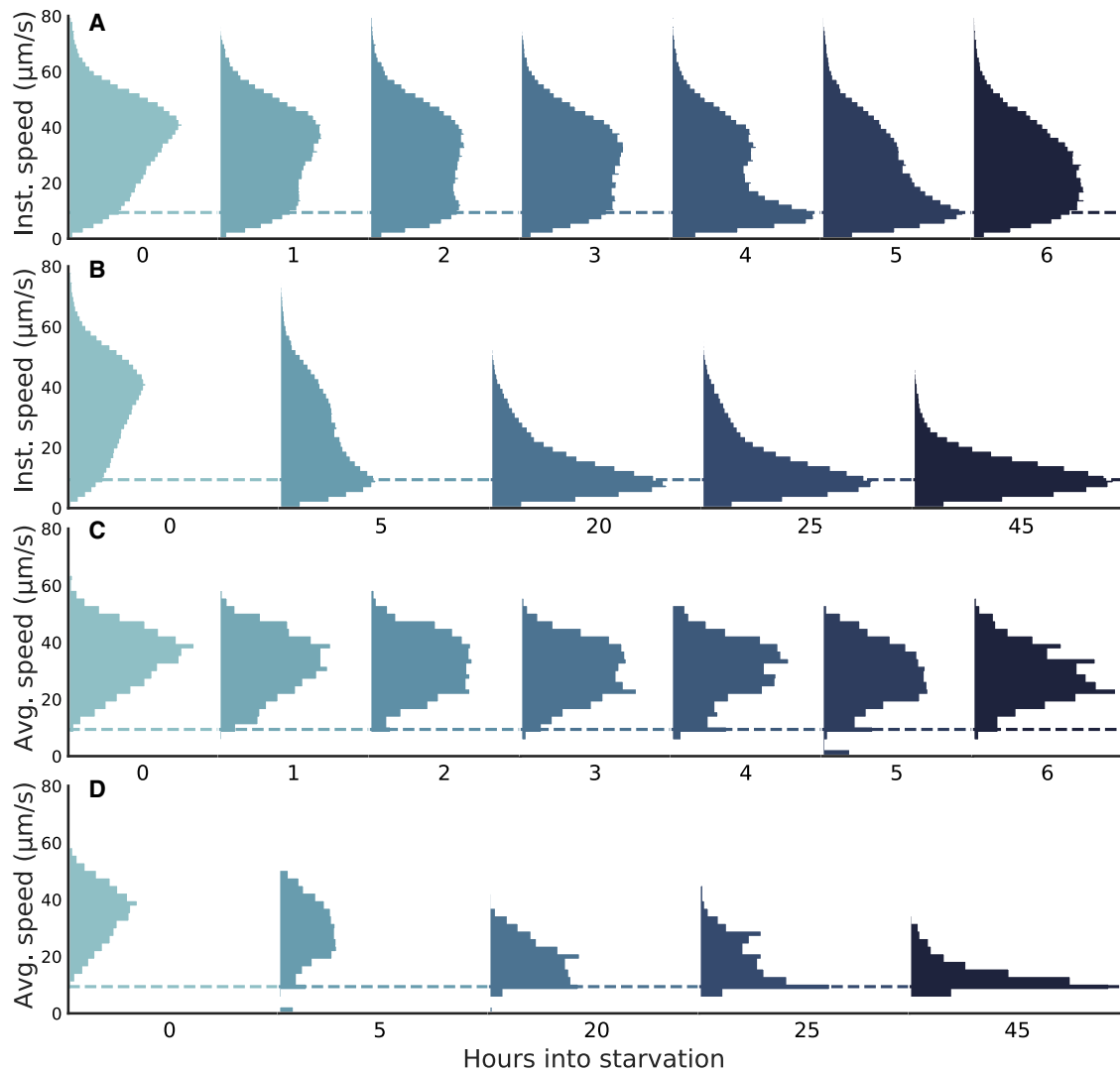
FIGURE 1 Under starvation conditions, the instantaneous and average speed distributions of *B. bacteriovorus* shift across time. (*A*) Instantaneous speed distributions are bimodal with a substantial shift toward an apparent diffusive state over the first 6 h. (*B*) Beyond hour 6 during starvation, the instantaneous speed distribution relaxes to a unimodal distribution about the expected diffusive speed for a Brownian particle of *B. bacteriovorus*' size ($\approx 9.40$ $\mu$m s$^{-1}$, *dashed lines*). (*C*) Distributions of speeds averaged over individual trajectories are largely unimodal over the first 6 h. (*D*) Average speed distributions over 45 h eventually relax to the expected diffusive speed. The sampling statistics for each histogram can be found in supporting material, sampling statistics for main text figures.

## Diffusive speed calculations

As mentioned before, Fig. 1 contains a bimodal instantaneous speed distribution with peaks at 10 and 40 $\mu$m s$^{-1}$. We interpret these peaks as a diffusive state and a swimming state, respectively. To justify our interpretation, we compare our inferred diffusive speed ($10$ $\mu$m s$^{-1}$) with the expected diffusive speed calculated using the Stokes-Einstein equation. Assuming the bacterium is a sphere, we can calculate the diffusion coefficient as given by the Stokes-Einstein equation:

$$D = \frac{kT}{6\pi\nu r}, \tag{1}$$

where $\nu$ is the dynamic viscosity and $r$ is the radius of the sphere. The dynamic viscosity of water at 28°C (the temperature of the incubator) is approximately $8.318 \times 10^{-4}$ kg m s$^{-1}$, and the radius of the bacterium is approximately $0.375$ $\mu$m. By substituting these values and Boltzmann's constant, $k$, the diffusion coefficient can be estimated as $0.707$ $\mu$m$^2$ s$^{-1}$. The exposure time, $\Delta t$, between two frames is $0.008$ s. Therefore, the diffusive speed is approximately $9.40$ $\mu$m s$^{-1}$, as given by:

$$v_{\text{diff}} = \sqrt{D/\Delta t} \tag{2}$$

whose outcome is consistent with our measurement.

As an aside, we can compare this to the diffusive speed of an *E. coli*. A rough calculation for *E. coli*'s diffusive speed can be obtained by approximating the cell as a sphere and taking its volume to be $\approx 1$ $\mu$m$^3$, giving a radius
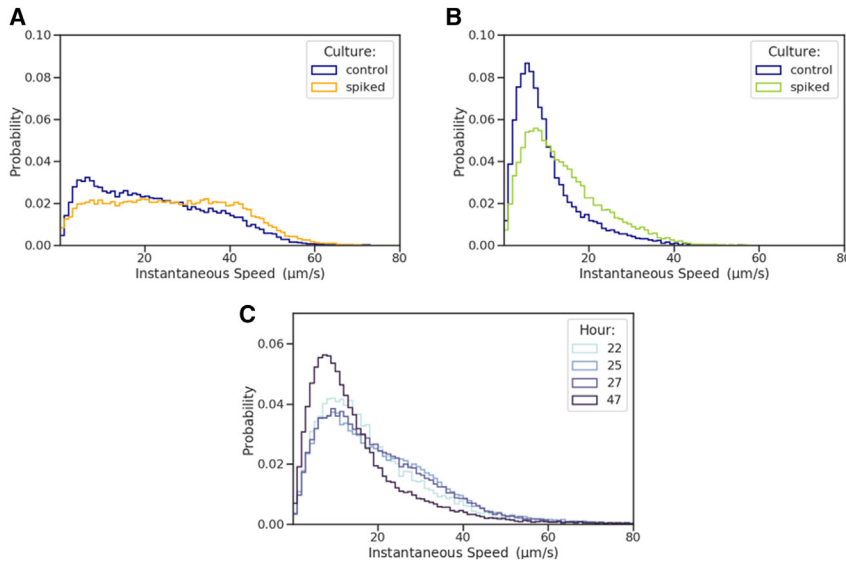
A

B



C

FIGURE 2 After addition of LB, *B. bacteriovorus* begins to swim more frequently even after long starvation times. We compare the instantaneous speed distributions of our control, starving *B. bacteriovorus* (*blue*), to that of cultures spiked with LB at hour 4 (*orange*) and hour 20 (*green*). Both spiked cultures were observed after 2 h of exposure. (*A*) After 2 h of exposure, the culture spiked at hour 4 (*orange*) exhibits a small repopulation of the active swimming speed peak. (*B*) After 2 h of exposure, the culture spiked at hour 20 (*green*) has faster speeds than the control (*blue*). (*C*) The culture spiked at hour 20 can be seen after several hours of exposure with negligible difference (21–26), indicating that, after several hours of exposure, the nutrients are in excess. The sampling statistics for each histogram can be found in supporting material, sampling statistics for main text figures.

of 0.6 $\mu$m. From Eq. 2 above, we get $v_{\mathrm{diff}} \approx 7.4$ $\mu$m s$^{-1}$. Considering the approximations made in this calculation, *E. coli*'s diffusive speed of 7.4 $\mu$m s$^{-1}$ is actually similar to the diffusive speed of *B. bacteriovorus*, which is approximately 9.4 $\mu$m s$^{-1}$.

### Starvation of *B. bacteriovorus*

Representative traces, exhibiting both active swimming states (*light blue*) and apparent diffusive states (*dark blue*) visited within individual trajectories, are shown in Fig. 3. As described in the materials and methods, hour 0 is observed 10 min after filtering.

In Fig. 1, we show the instantaneous and average speed distributions as a function of age. Starting from hour 0, the instantaneous speeds exhibit a bimodal distribution, with peaks around 10 and 40 $\mu$m s$^{-1}$. The former peak is centered around the expected diffusive speed of a spherical particle the *B. bacteriovorus*' size, as predicted by the Stokes-Einstein relation (Fig. 1, *dashed line*) (see the previous section for calculation).

As bacteria age over the first 6 h under starvation conditions, we observe a decrease in the higher-speed population and an increase in the apparent diffusive population of our bimodal distribution. The observed shifts suggest the possibility that the bacteria are actively adjusting the amount of time spent swimming in response to persisting starvation conditions. The evolution of the speed distribution, from hour 0 up to hour 45, is shown in Fig. 1 *B* (with bimodality shifting to unimodality around the 20-h mark). In the materials and methods, we describe tracking details.

We highlight that, by contrast to *B. bacteriovorus* which continues swimming for hours poststarvation, *E. coli* stops swimming as soon as we can image it when under starvation as shown in Fig. S1.

To determine whether there are two bacterial populations or two motility states for each bacterium contributing to the bimodal instantaneous distributions (Fig. 1, *A* and *B*), the average velocity over each bacterium's trajectory was calculated (Fig. 1 *C*). The speed distributions have a similar average velocity over the first 6 h. This indicates that the speed of each bacterium is more similar to that of other bacteria than the speeds sampled within its own trajectory. Indeed the instantaneous speed distribution at hour 6 appears to shift slightly toward higher values compared with hour 5 (see Fig. 1 *A*). We attribute this shift to noise, for two reasons 1) the width of the distribution at hour 6 is generally consistent with that of previous hours and 2) the number of live bacteria decreases at later hours, resulting in poorer statistical accuracy. However, just as before, the average velocity approaches the expected diffusive speed after hour 20 (Fig. 1 *D*, *dashed line*), suggesting that *B. bacteriovorus* are apparently diffusing. The absence of a well-defined unimodal speed distribution is corroborated by direct visual inspection of bacterial trajectories; representative traces, exhibiting both active swimming and apparent diffusive states within individual trajectories, are shown in Fig. 3. Additional runs can be found in the supporting material (Figs. S8–S10).

To demonstrate that the observations depicted in Fig. 1 are not an artifact of the localization method employed, we also performed deep learning localization on the same data sets and obtained consistent results. Furthermore, we conducted Gaussian mixture fitting and provide a list of all fitted parameters. These results are presented in the supporting material, comparison to another analysis method.

### Spiking of *B. bacteriovorus*

Following up on the preanalysis, we exposed previously starving bacteria to nutrient-rich medium (LB), as described
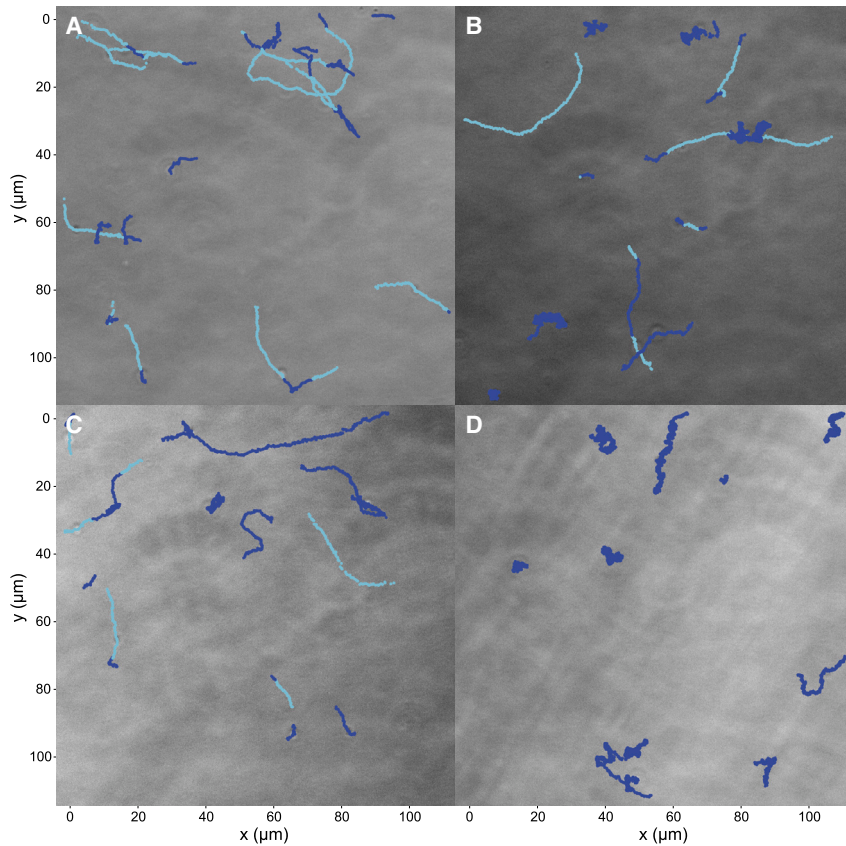
FIGURE 3  Representative *B. bacteriovorus* trajectories depicting instantaneous velocities. Bacterial trajectories are obtained for the first 500 frames at hour 0 (*A*), hour 4 (*B*), hour 6 (*C*), and hour 20 (*D*). Trajectories are colored according to the state at that time level (active swimming is bright and apparent diffusive is dark) determined by thresholding above and below 30 $\mu$m/s. This threshold is selected based on the midpoint of the center of both peaks in the bimodal distribution in Fig. 1.

in the materials and methods. One of the main ingredients, yeast extract, has been shown to induce an active chemotactic response in *B. bacteriovorus* (11). In Fig. 2, we compare the motile response to the addition of LB with a control where *B. bacteriovorus* is kept in nutrient-poor medium (HM), identical to those in Fig. 1.

To determine if *B. bacteriovorus* is revivable, we took a *B. bacteriovorus* culture and separated it into three. One of these cultures was spiked with LB at hour 4, another was spiked with LB at hour 20, and the third was never spiked. The spiked cultures remained in the LB solution for the duration of the remainder of the experiment. For both spiked cultures, we then looked at their instantaneous speed distributions after 2 h of exposure, thus at hour 6 for Fig. 2 *A* and at hour 22 for Fig. 2 *B*. We found that bacteria move more frequently after spiking. Additional runs are provided in Figs. S11 and S12.

As seen in Fig. 2 *C*, after leaving the bacteria in the spiked rich medium, their speed distributions did not greatly vary, indicating that over several hours there is an excess of nutrients. To further determine if the concentration of LB used to spike the cultures at hour 4 and hour 20 had an overall effect on the speed distributions, we spiked cultures at half the concentration of LB used to spike the cultures as well as at 10× the concentration (see Fig. S13). The half LB spiked cultures exhibited similar results to the initial whole concen-

tration seen in Fig. 2. At 10× LB, the speed of *B. bacteriovorus* was observed to be slower. This can be attributed to the higher osmolarity of the solution, consistent with previous reports in the literature (60). Although high osmolarity is known to generally lower fitness (61), the exact mechanism by which higher osmolarities lead to slower *B. bacteriovorus* speeds is yet to be fully understood (60). One recent explanation suggests that higher osmolarities can impede the metabolism of *B. bacteriovorus* and hinder the regeneration of NADH pools, without necessarily causing cell death (62).

Spiking *B. bacteriovorus* at hour 40 resulted in no change compared with the starving control (Figs. S14 and S15). This indicates that, although the speed distribution in Fig. 1 looks similar for hours 20 and 45, the bacteria cannot be revived after hour 45.

These findings then naturally beg the question as to whether *B. bacteriovorus* recovers its bimodal behavior after reinitialization of starvation conditions (resuspension in HM) after spiking. Here, we follow up on the spiking experiments (Fig. 2), except that after spiking we centrifuged *B. bacteriovorus* and resuspended them in nutrient-poor medium. We then ask how the fraction of swimming versus apparently diffusing *B. bacteriovorus* differ from our control (Fig. S7). Qualitatively, we find that the bacteria continue to spend more time swimming compared with

the control—regardless of the tendency of centrifugation to slow down *B. bacteriovorus* (see Fig. S2)—suggesting that there is some degree of memorylessness. In other words, these results suggest that *B. bacteriovorus* behave as if they were exposed to rich medium and starved for the very first time.

## DISCUSSION

Bimodality in the instantaneous speed distributions over the first 6 h under starvation (Fig. 1, *A* and *B*), along with the absence of bimodality in the trajectory-averaged speed distributions (Fig. 1, *C* and *D*), suggests that *B. bacteriovorus* samples both active swimming and apparent diffusive states of motility *within* the course of a single trajectory. At any given time point (after the initiation of starvation), the motile behavior of a given *B. bacteriovorus* appears to be representative of other cells within the population. Indeed, *B. bacteriovorus* cells sample speeds from a bimodal distribution, with active swimming and apparent diffusive states, from the onset of starvation.

*B. bacteriovorus* remains active over hours and our spiking experiments not only show that *B. bacteriovorus* can be resuscitated after even 20 h of starvation, but that those bacteria that *do* stop swimming (and revert to apparent diffusion) can be stimulated back into sampling the high-speed state of its velocity distribution. Indeed, shortly after spiking, *B. bacteriovorus* increases the fraction of time it spends swimming. As the reinitiation of starvation conditions (Fig. S7) produced behavior similar to initial starvation, it is likely that *B. bacteriovorus* allocates energy reserves for active motion in direct response to its environment, regardless of previous conditions, and that the *B. bacteriovorus* population eventually enters an energy-conserving apparent diffusive state if starved for long enough. Previous studies in which bimodal speed distributions are observed are normally associated with the bundling of flagella for peritrichously flagellated species (e.g., the run-and-tumble paradigm (56,63)), which is not a feasible mechanism for the uniflagellated *B. bacteriovorus* and occurs on second timescales far shorter than the hours and days timescales involved in reweighting motility states.

The subtle way in which *B. bacteriovorus* modulates which of the states of its speed distribution it samples is worthy, in and of itself, of future molecular attention. This is especially meaningful in light of the stark contrast in its ability to keep swimming under starvation compared with its prey, *E. coli*. To wit, it is already known that *B. bacteriovorus* dramatically varies its gene expression levels between attack and growth phases (57,64,65) with, most recently, work exploring *B. bacteriovorus*' motility reduction under starvation linked to cyclic-di-GMP effectors playing the role of "motility brakes" (66).

These findings, in turn, beg broader questions associated with the cost, both hydrodynamic and transcriptional, tied to

motility reinitiation by *B. bacteriovorus*. Our work here provides a piece of the puzzle toward assessing the energetic cost associated with motility with time from the onset of starvation. It remains to be seen whether, in the end, active swimming state modulation with age is tied to transcriptional activity and part of a global strategy to jointly minimize hydrodynamic and transcriptional energy expenditure to maximize the probability of locating prey.

## DATA AVAILABILITY

*B. bacteriovorus* localization data are available at statphysbio.physics. asu.edu.

## SUPPORTING MATERIAL

Supporting material can be found online at https://doi.org/10.1016/j.bpj. 2023.06.008.

## AUTHOR CONTRIBUTIONS

L.W.Q.X. and J.S.B. performed all of the analysis. S.P. oversaw all aspects of the research.

## ACKNOWLEDGMENTS

## DECLARATION OF INTERESTS

The authors have no conflicts of interest to declare.

## REFERENCES

1. Drescher, K., J. Dunkel, …, R. E. Goldstein. 2011. Fluid dynamics and noise in bacterial cell-cell and cell-surface scattering. *Proc. Natl. Acad. Sci. USA.* 108:10940–10945.

2. Jashnsaz, H., M. Al Juboori, …, S. Pressé. 2017. Hydrodynamic Hunters. *Biophys. J.* 112:1282–1289. https://doi.org/10.1016/j.bpj. 2017.02.011.

3. Meng, Y., Y. Li, …, H. C. Hoch. 2005. Upstream migration of *Xylella fastidiosa* via pilus-driven twitching motility. *J. Bacteriol.* 187:5560–5567.

4. Shen, Y., A. Siryaporn, …, H. A. Stone. 2012. Flow directs surface-attached bacteria to twitch upstream. *Biophys. J.* 103:146–151.

5. Kaya, T., and H. Koser. 2012. Direct upstream motility in *Escherichia coli"*. *Biophys. J.* 102:1514–1523.

6. Baker, M. D., P. M. Wolanin, and J. B. Stock. 2006. Signal transduction in bacterial chemotaxis. *Bioessays.* 28:9–22. https://doi.org/10.1002/bies.20343.

7. Dori-Bachash, M., B. Dassa, E. Jurkevitch…, 2008. Proteome-based comparative analyses of growth stages reveal new cell cycle-dependent

functions in the predatory bacterium *Bdellovibrio bacteriovorus*. *Appl. Environ. Microbiol.* 74:7152–7162. https://doi.org/10.1128/AEM.01736-08.

8. Waters, C. M., and B. L. Bassler. 2005. Quorum Sensing: Cell-to-Cell Communication in Bacteria. *Annu. Rev. Cell Dev. Biol.* 21:319–346. https://doi.org/10.1146/annurev.cellbio.21.012704.131001.

9. Mukherjee, S., S. C. Seok, …, J. Das. 2013. Data-driven quantification of the robustness and sensitivity of cell signaling networks. *Phys. Biol.* 10, 066002.

10. Jiang, L., Q. Ouyang, and Y. Tu. 2010. Quantitative Modeling of *Escherichia coli* Chemotactic Motion in Environments Varying in Space and Time. *PLoS Comput. Biol.* 6, e1000735.

11. LaMarre, A. G., S. C. Straley, and S. F. Conti. 1977. Chemotaxis toward amino acids by *Bdellovibrio bacteriovorus*. *J. Bacteriol.* 131:201–207.

12. Hespell, R. B., M. F. Thomashow, and S. C. Rittenberg. 1974. Changes in cell composition and viability of *Bdellovibrio bacteriovorus* during starvation. *Arch. Microbiol.* 97:313–327. https://doi.org/10.1007/bf00403070.

13. Dashiff, A., R. A. Junka, …, D. E. Kadouri. 2011. Predation of human pathogens by the predatory bacteria *Micavibrio aeruginosavorus* and *Bdellovibrio bacteriovorus*". *J. Appl. Microbiol.* 110:431–444.

14. Sockett, R. E., and C. Lambert. 2004. *Bdellovibrio* as therapeutic agents: a predatory renaissance? *Nat. Rev. Microbiol.* 2:669–675.

15. Kadouri, D., and G. A. O'Toole. 2005. Susceptibility of biofilms to *Bdellovibrio bacteriovorus* attack. *Appl. Environ. Microbiol.* 71:4044–4051.

16. Passino, K. M. 2002. Biomimicry of bacterial foraging for distributed optimization and control. *Control Syst. Mag.* 22:52–67.

17. Astling, D. P., J. Y. Lee, and D. R. Zusman. 2006. Differential effects of chemoreceptor methylation-domain mutations on swarming and development in the social bacterium *Myxococcus xanthus*. *Mol. Microbiol.* 59:45–55. https://doi.org/10.1111/j.1365-2958.2005.04926.x.

18. Williams, H. N., J. I. Kelley, …, B. F. Turng. 1995. The association of *Bdellovibrios* with surfaces in the aquatic environment. *Can. J. Microbiol.* 41:1142–1147.

19. Lambert, C., A. K. Fenton, …, R. E. Sockett. 2011. Predatory *Bdellovibrio* Bacteria Use Gliding Motility To Scout for Prey on Surfaces. *J. Bacteriol.* 193:3139–3141.

20. Harini, K., V. Ajila, and S. Hegde. 2013. Bdellovibrio Bacteriovorus: A Future Antimicrobial Agent?. https://doi.org/10.4103/0972-124X.124534.

21. Chanyi, R. M., and S. F. Koval. 2014. Role of Type IV Pili in Predation by *Bdellovibrio bacteriovorus*". *PLoS One.* 9:e113404. https://doi.org/10.1371/journal.pone.0113404.

22. Straley, S. C., and S. F. Conti. 1977. Chemotaxis by *Bdellovibrio bacteriovorus* toward prey. *J. Bacteriol.* 132:628–640.

23. Oyedara, O. O., E. d. J. De Luna-Santillana, …, M. A. Rodriguez-Perez. 2016. Isolation of *Bdellovibrio sp.* from soil samples in Mexico and their potential applications in control of pathogens. *MicrobiologyOpen.* 5:992–1002.

24. Yu, R., S. Zhang, …, C. Li. 2017. Isolation and application of predatory *Bdellovibrio*-and-like organisms for municipal waste sludge biolysis and dewaterability enhancement. *Front. Environ. Sci. Eng.* 11:10.

25. Sun, Y., J. Ye, …, T. Zhou. 2017. Predation Efficacy of *Bdellovibrio bacteriovorus* on Multidrug-Resistant Clinical Pathogens and Their Corresponding Biofilms. *Jpn. J. Infect. Dis.* 70:485–489. https://doi.org/10.7883/yoken.JJID.2016.405.

26. Iebba, V., V. Totino, …, M. Artini. 2014. Bdellovibrio bacteriovorus directly attacks Pseudomonas aeruginosa and Staphylococcus aureus cystic fibrosis isolates. *Front. Microbiol.* 5. https://doi.org/10.3389/fmicb.2014.00280.

27. Shatzkes, K., E. Singleton, …, D. E. Kadouri. 2016. Predatory Bacteria Attenuate *Klebsiella pneumoniae* Burden in Rat Lungs. *mBio.* 7, e01847-16. https://doi.org/10.1128/mBio.01847-16.

28. Atterbury, R. J., L. Hobley, …, R. E. Sockett. 2011. Effects of orally administered *Bdellovibrio bacteriovorus* on thewell-being and *Salmonella* colonization of young chicks. *Appl. Environ. Microbiol.* 77:5794–5803.

29. Romanowski, E. G., N. A. Stella, …, R. M. Q. Shanks. 2016. Predatory bacteria are nontoxic to the rabbit ocular surface. *Sci. Rep.* 6, 30987.

30. Willis, A. R., C. Moore, …, R. E. Sockett. 2016. Injections of Predatory Bacteria Work Alongside Host Immune Cells to Treat *Shigella* Infection in Zebrafish Larvae. *Curr. Biol.* 26:3343–3351.

31. Park, S., D. Kim, …, T. Kim. 2011. A microfluidic concentrator array for quantitative predation assays of predatory microbes. *Lab Chip.* 11:2916–2923. https://doi.org/10.1039/c1lc20230h.

32. Van Essche, M., M. Quirynen, …, W. Teughels. 2009. *Bdellovibrio bacteriovorus* attacks *Aggregatibacter actinomycetemcomitans*". *J. Dent. Res.* 88:182–186. https://doi.org/10.1177/0022034508329693.

33. Mitchell, R., S. Yankfsky, and H. W. Jannasch. 1967. Lysis of *Escherichia coli* by marine micro-organisms. *Nature.* 215:891–893. https://doi.org/10.1038/215891a0.

34. Lambert, C., M. C. M. Smith, and R. E. Sockett. 2003. A novel assay to monitor predator-prey interactions for *Bdellovibrio bacteriovorus* 109 J reveals a role for methyl-accepting chemotaxis proteins in predation. *Environ. Microbiol.* 5:127–132. https://doi.org/10.1046/j.1462-2920.2003.00385.x.

35. Rendulic, S., P. Jagtap, …, S. C. Schuster. 2004. A predator unmasked: life cycle of *Bdellovibrio bacteriovorus* from a genomic perspective. *Science.* 303:689–692. https://doi.org/10.1126/science.1093027.

36. Steyert, S. R., and S. A. Pineiro. 2007. Development of a novel genetic system to create markerless deletion mutants of *Bdellovibrio bacteriovorus*". *Appl. Environ. Microbiol.* 73:4717–4724. https://doi.org/10.1128/AEM.00640-07.

37. Lambert, C., K. J. Evans, …, R. E. Sockett. 2006. Characterizing the flagellar filament and the role of motility in bacterial prey-penetration by *Bdellovibrio bacteriovorus*". *Mol. Microbiol.* 60:274–286. https://doi.org/10.1111/j.1365-2958.2006.05081.x.

38. Lambert, C., K. A. Morehouse, …, R. E. Sockett. 2006. Bdellovibrio: growth and development during the predatory cycle. *Curr. Opin. Microbiol.* 9:639–644. https://doi.org/10.1016/j.mib.2006.10.002.

39. Thomashow, M. F., and T. W. Cotter. 1992. *Bdellovibrio* host dependence: the search for signal molecules and genes that regulate the intraperiplasmic growth cycle. *J. Bacteriol.* 174:5767–5771. https://doi.org/10.1128/jb.174.18.5767-5771.1992.

40. Fratamico, P. M., and R. C. Whiting. 1995. Ability of *Bdellovibrio bacteriovorus* 109J to Lyse Gram-Negative Food-Borne Pathogenic and Spoilage Bacteria. *J. Food Prot.* 58:160–164. https://doi.org/10.4315/0362-028X-58.2.160.

41. Seidler, R. J., and M. P. Starr. 1969. Factors affecting the intracellular parasitic growth of *Bdellovibrio bacteriovorus* developing within *Escherichia coli*". *J. Bacteriol.* 97:912–923.

42. Stolp, H., and H. Petzold. 1962. Untersuchungen ueber einen obligat parasitishen Mikroorganismus mit lyticher Aktivitaet fuer Pseudomonas-bakterien. *Phytopathology.* 45:364–390.

43. Stolp, H., and M. P. Starr. 1963. *Bdellovibrio bacteriovorus gen. et sp. n.*, a predatory, ectoparasitic, and bacteriolytic microorganism. *Antonie Leeuwenhoek.* 29:217–248.

44. Seidler, R. J., and M. P. Starr. 1969. Isolation and Characterization of Host-Independent *Bdellovibrios*". *J. Bacteriol.* 100:769–785.

45. Varon, M., and B. P. Zeigler. 1978. Bacterial predator-prey interaction at low prey density. *Appl. Environ. Microbiol.* 36:11–17.

46. Lambert, C., L. Hobley, …, L. Sockett. 2009. A predatory patchwork: membrane and surface structures of *Bdellovibrio bacteriovorus*". *Adv. Microb. Physiol.* 54:313–361.

47. Straley, S. C., and S. F. Conti. 1974. Chemotaxis by *Bdellovibrio bacteriovorus*". *J. Bacteriol.* 120:549–551.

48. Strauch, E., D. Schwudke, and M. Linscheid. 2007. Predatory mechanisms of *Bdellovibrio* and like organisms. *Future Microbiol.* 2:63–73. https://doi.org/10.2217/17460913.2.1.63.

49. Drescher, K., R. E. Goldstein, …, I. Tuval. 2010. Direct Measurement of the Flow Field around Swimming Microorganisms. *Phys. Rev. Lett.* 105, 168101.

50. Lushi, E., H. Wioland, and R. E. Goldstein. 2014. Fluid flows created by swimming bacteria drive self-organization in confined suspensions. *Proc. Natl. Acad. Sci. USA.* 111:9733–9738.

51. Frymier, P. D., R. M. Ford, …, P. T. Cummings. 1995. Three-dimensional tracking of motile bacteria near a solid planar surface. *Proc. Natl. Acad. Sci. USA.* 92:6195–6199.

52. Lauga, E., W. R. DiLuzio, …, H. A. Stone. 2006. Swimming in Circles: Motion of Bacteria near Solid Boundaries. *Biophys. J.* 90:400–412.

53. Di Leonardo, R., D. Dell'Arciprete, …, V. Iebba. 2011. Swimming with an Image. *Phys. Rev. Lett.* 106, 038101.

54. Hu, J., A. Wysocki, …, G. Gompper. 2015. Physical sensing of surface properties by microswimmers: directing bacterial motion via wall slip. *Sci. Rep.* 5, 9586.

55. Matz, C., and S. Kjelleberg. 2005. Off the hook–how bacteria survive protozoan grazing. *Trends Microbiol.* 13:302–307.

56. Matz, C., and K. Jürgens. 2005. High motility reduces grazing mortality of planktonic bacteria. *Appl. Environ. Microbiol.* 71:921–929.

57. Karunker, I., O. Rotem, …, R. Sorek. 2013. A global transcriptional switch between the attack and growth forms of Bdellovibrio bacteriovorus. *PLoS One.* 8:e61850. https://doi.org/10.1371/journal.pone.0061850.

58. Lambert, C., T. R. Lerner, …, R. E. Sockett. 2016. Interrupting peptidoglycan deacetylation during *Bdellovibrio* predator-prey interaction prevents ultimate destruction of prey wall, liberating bacterial-ghosts. *Sci. Rep.* 6:26010. https://doi.org/10.1038/srep26010.

59. Allan, D., T. Caswell, …, C. M. van der Wel. 2019. soft-matter/trackpy: Trackpy v0.4.2. Version v0.4.2. Preprint at Zendo. https://doi.org/10.5281/zenodo.3492186.

60. Hansol, I., S. Son, …, C. M. Ghim. 2017. Serum albumin and osmolality inhibit *Bdellovibrio bacteriovorus* predation in human serum. *Sci. Rep.* 7:2045–2322. https://doi.org/10.1038/s41598-017-06272-2.

61. Ghosh, K., A. M. R. de Graff, …, K. A. Dill. 2016. Role of proteome physical chemistry in cell behavior. *J. Phys. Chem. B.* 120:9549–9563.

62. Jang, H., W. Mun, …, R. J. Mitchell. 2022. Use of Resazurin To Rapidly Enumerate Bdellovibrio and Like Organisms and Evaluate Their Activities. *Microbiol. Spectr.* 10:e0082522.

63. Toley, B. J., and N. S. Forbes. 2012. Motility is critical for effective distribution and accumulation of bacteria in tumor tissue. *Integr. Biol.* 4:165–176.

64. Waso, M., S. Khan, …, W. Khan. 2020. Expression of attack and growth phase genes of *Bdellovibrio bacteriovorus* in the presence of Gram-negative and Gram-positive prey. *Microbiol. Res.* 235:126437. https://doi.org/10.1016/j.micres.2020.126437.

65. Herencias, C., S. Salgado-Briegas, …, J. Nogales. 2020. Providing new insights on the byphasic lifestyle of the predatory bacterium *Bdellovibrio bacteriovorus* through genome-scale metabolic modeling. *PLoS Comput. Biol.* 16, e1007646.

66. Sathyamoorthy, R., Y. Kushmaro, …, E. Jurkevitch. 2020. To hunt or to rest: prey depletion induces a novel starvation survival strategy in bacterial predators. *ISME J.* 15:109–123.

# Supplemental information

# Two-state swimming: Strategy and survival of a model bacterial predator in response to environmental cues

**Lance W.Q. Xu (徐伟青), J. Shepard Bryan IV, Zeliha Kilic, and Steve Pressé**

# Two state swimming: strategy and survival of a model bacterial predator in response to environmental cues

Lance W.Q. Xu (徐伟青)[1,2], J. Shepard Bryan IV[1,2], Zeliha Kilic[3], and Steve Pressé[1,2,4,*]

[1]Department of Physics, Arizona State University, Tempe, AZ
[2]Center for Biological Physics, Arizona State University, Tempe, AZ
[3]Single-Molecule Imaging Center, Saint Jude's Children Hospital, Memphis, TN
[4]School of Molecular Sciences, Arizona State University, Tempe, AZ
[*]spresse@asu.edu

## SUPPLEMENTARY INFORMATION

## Supplementary Figures
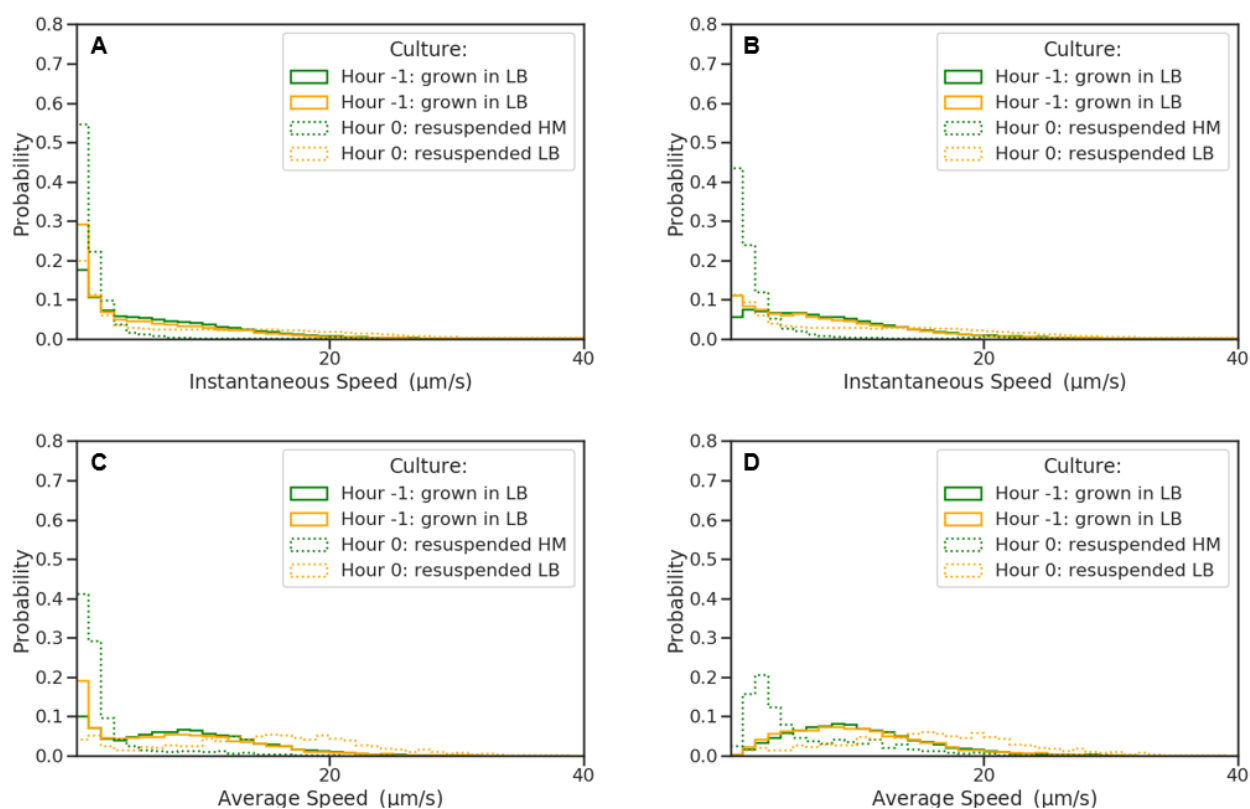


Figure S1: *E. coli* **immediately decreases its speed under starvation conditions.** Two runs were conducted in which each *E. coli* culture was grown in LB (Hour -1) and either resuspended in HM (green) or LB (orange) at Hour 0. (A) The culture resuspended in HM (Hour 0, dotted green) had an increase in population of instantaneous slow speeds as compared to before starvation (Hour -1, solid green). (B) The motile trajectories (at least one instantaneous speed within the trajectory above $5\,\mu\mathrm{m\,s}^{-1}$) of *E. coli* have broader instantaneous speed distributions before centrifugation (Hour -1, solid orange and green) and after resuspension in LB (Hour 0, orange dotted) as compared to the starved culture (Hour 0, dotted green). (C) The culture resuspended in HM (Hour 0, dotted green) had an increase in population of average slow speeds as compared to prior to starvation (Hour -1, solid green) and the culture resuspended in LB (dotted orange). (D) The motile trajectories of *E. coli* have broader average speed distributions before centrifugation (Hour -1, solid orange and green) and after resuspension in LB (Hour 0, orange dotted) as compared to the starved culture (Hour 0, dotted green).
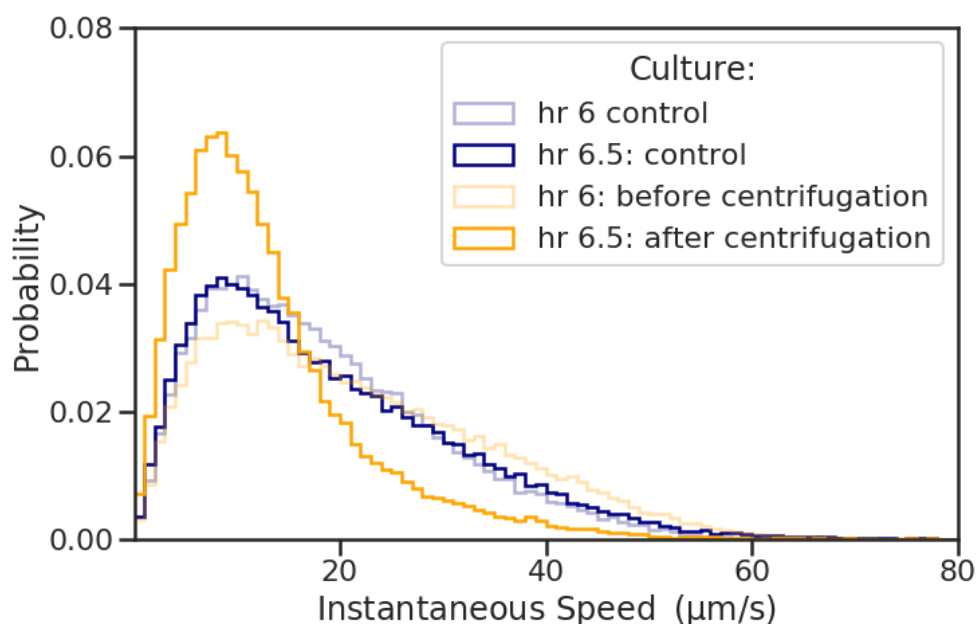
Figure S2: **There is an increase in the apparent diffusive state population after centrifugation.** A *B. bacteriovorus* culture starved for 6 hours was split as seen in the spiking experiments. One culture was not centrifuged (blue) while the other was centrifuged (orange) as discussed in the Methods section. There is no noticeable change between the control (blue) at Hour 6 and Hour 6.5. However, there is an increase in the apparent diffusive population after centrifugation (orange).
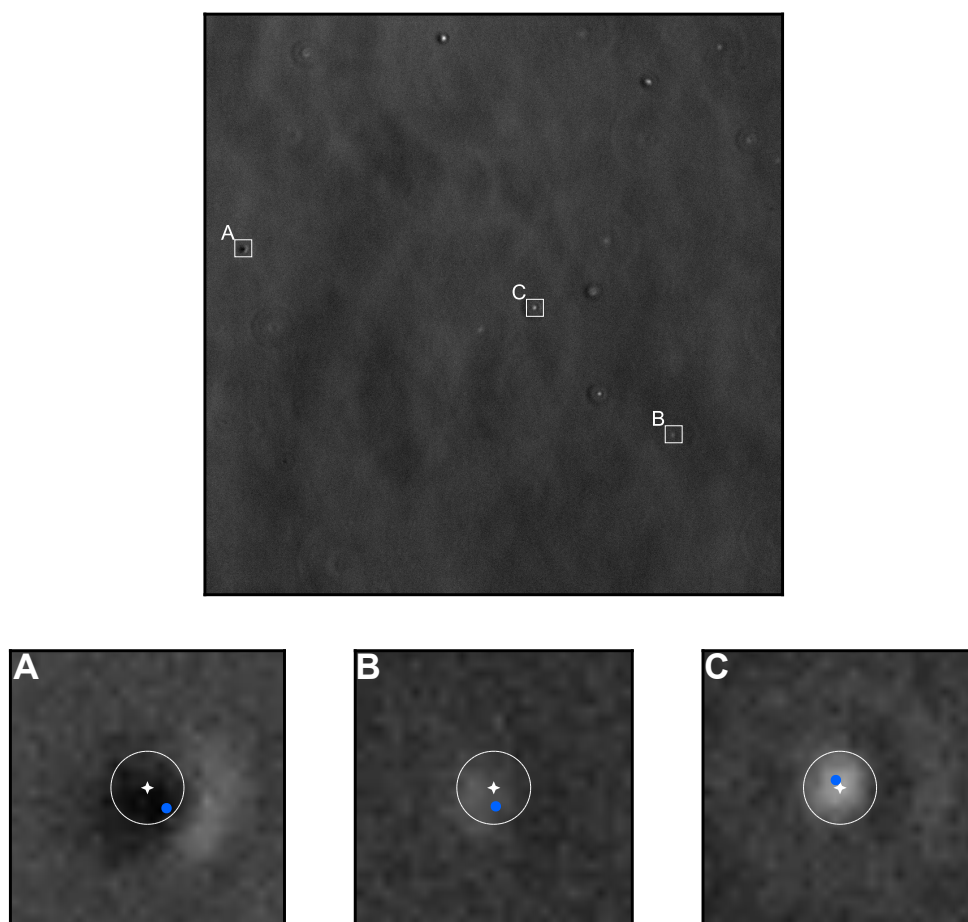
Figure S3: **Localization errors in the analysis of *B. bacteriovorus* datasets.** We selected a frame (1024x1024 pixels, 8 ms) containing multiple *B. bacteriovorus* from inverted phase contrast images. Three 30x30 pixel regions were then selected and presented in panels A-C. The ground truth *B. bacteriovorus* locations, annotated by eye, are denoted by a white star, while the automated (neural net) localization is indicated by a blue dot. The average error between our automated localizations and the hand-annotated localizations across all frames that have been manually annotated is denoted by a circle. The circle's radius represents our localization error.
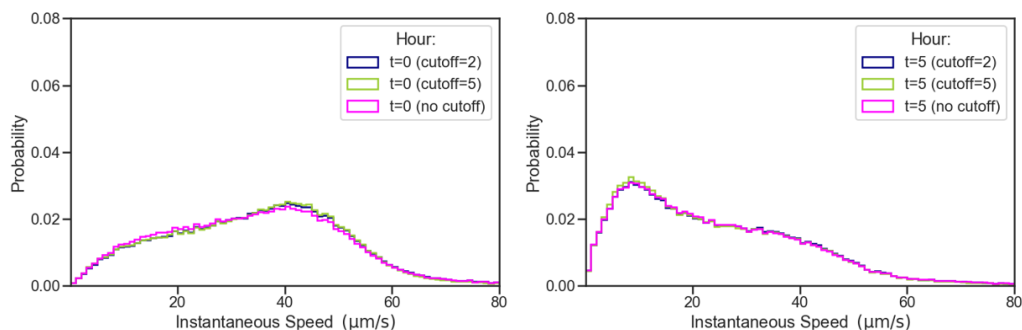
Figure S4: **Varying cutoffs of endpoints of trajectories does not affect the bimodal distribution**. From S1, the relative biases of cutting off different endpoints was seen for Hour 0. However, looking at the distributions after removing these frames from each trajectory, there is no noticeable effect on the structure of the bimodal distributions.
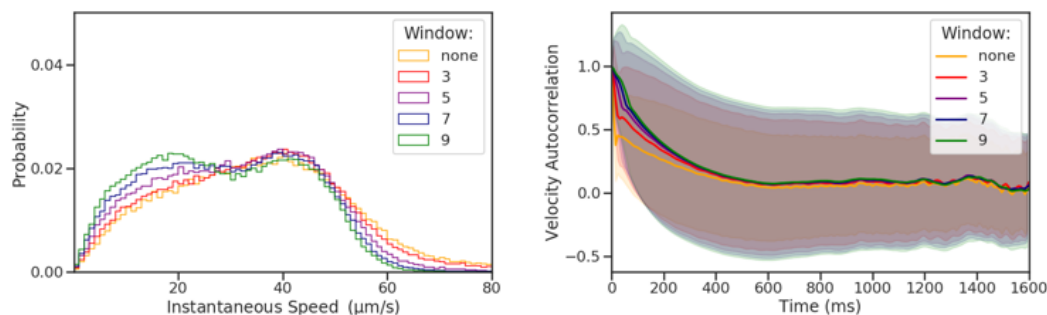


Figure S5: **Using different window averaging has minimal affects on the speed distribution and velocity autocorrelations.** The bimodal distribution for Hour 0 seen in figure 1 was observed using different window averaging. Overall a larger window causes the speed distributions to shift slightly to the left, but the overall distribution shape remains the same. The velocity autocorrelation is very similar regardless of the window. The histogram data was divided into 100 evenly spaced bins.
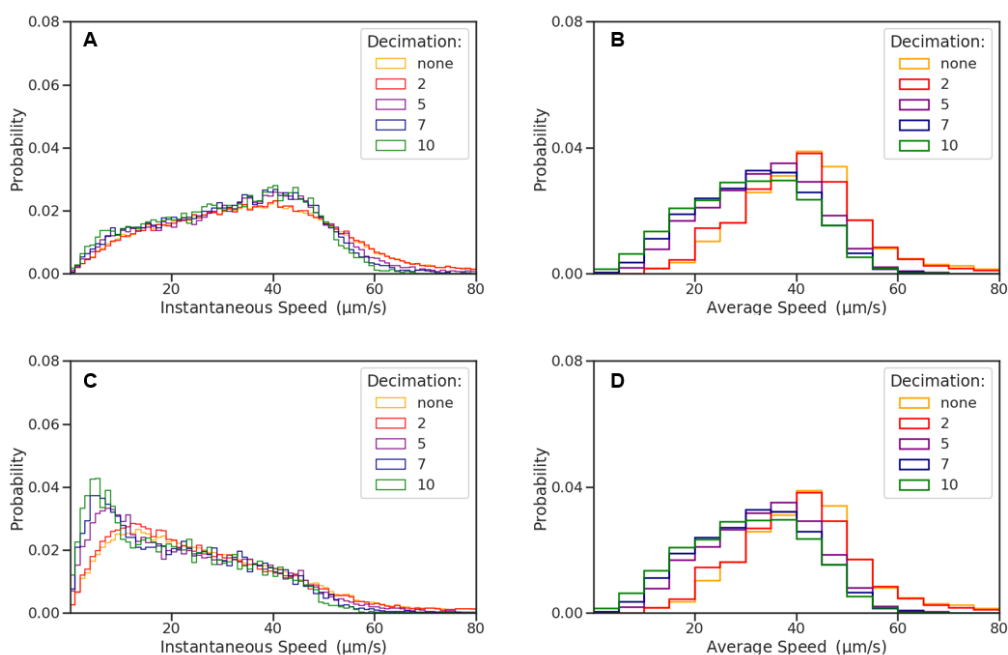
Figure S6: **Decimating the data has minor effects in the speed distributions.** To further test the bimodal behavior seen at early hours of starvation, the data was decimated. For example, for a decimation of 5, every fifth data point of a trajectory was used, thus also decreasing the number of samples. (A) Decimating the data does not show a noticeable effect even as much as taking only every tenth instantaneous speed of a bacterial trajectory at Hour 0. (B) A slight shift to a slower average speed is seen when utilizing fewer data points, but the overall shape of the distribution does not vary greatly at Hour 0. (C) Decimating the data at Hour 5 has an increase in the height of the apparent diffusive peak when taking every fifth to tenth data points. (D) The average speed distributions also show a shift to the left at Hour 5 with larger decimations. As the number of data points is less for Hour 5 compared with Hour 0, this may be a cause for further effects of using larger decimations (fewer data points). All data in the instantaneous speed and average speed histograms was divided into 100 and 30 evenly spaced bins, respectively.
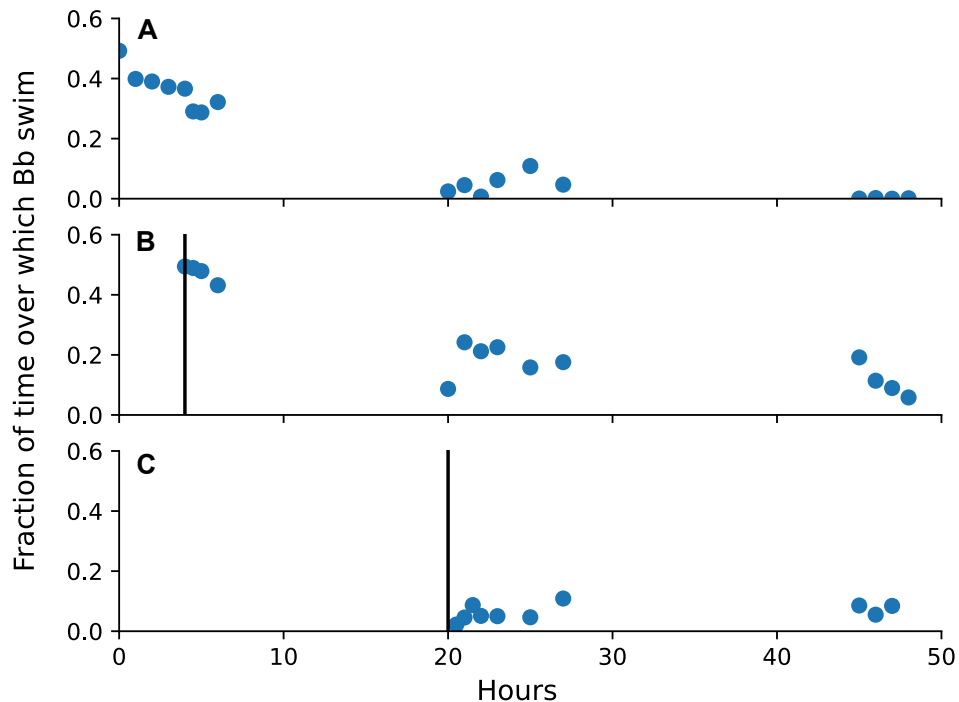
Figure S7: **Fraction of time over which *B. bacteriovorus* swim.** Here we plot the fraction of the *B. bacteriovorus* population swimming over time for our three experiments (no spiking, spiking at Hour 4, and spiking at Hour 20). We determine the fraction of *B. bacteriovorus* that are swimming by thresholding their speeds around 30$\mu$m/s, which is the midpoint line between the two speed peaks in figure 1. The top panel shows the control, the middle panel shows the *B. bacteriovorus* that have been spiked at Hour 4, and the bottom panel shows the *B. bacteriovorus* that have been spiked at Hour 20. Black vertical lines represent the spiking time.
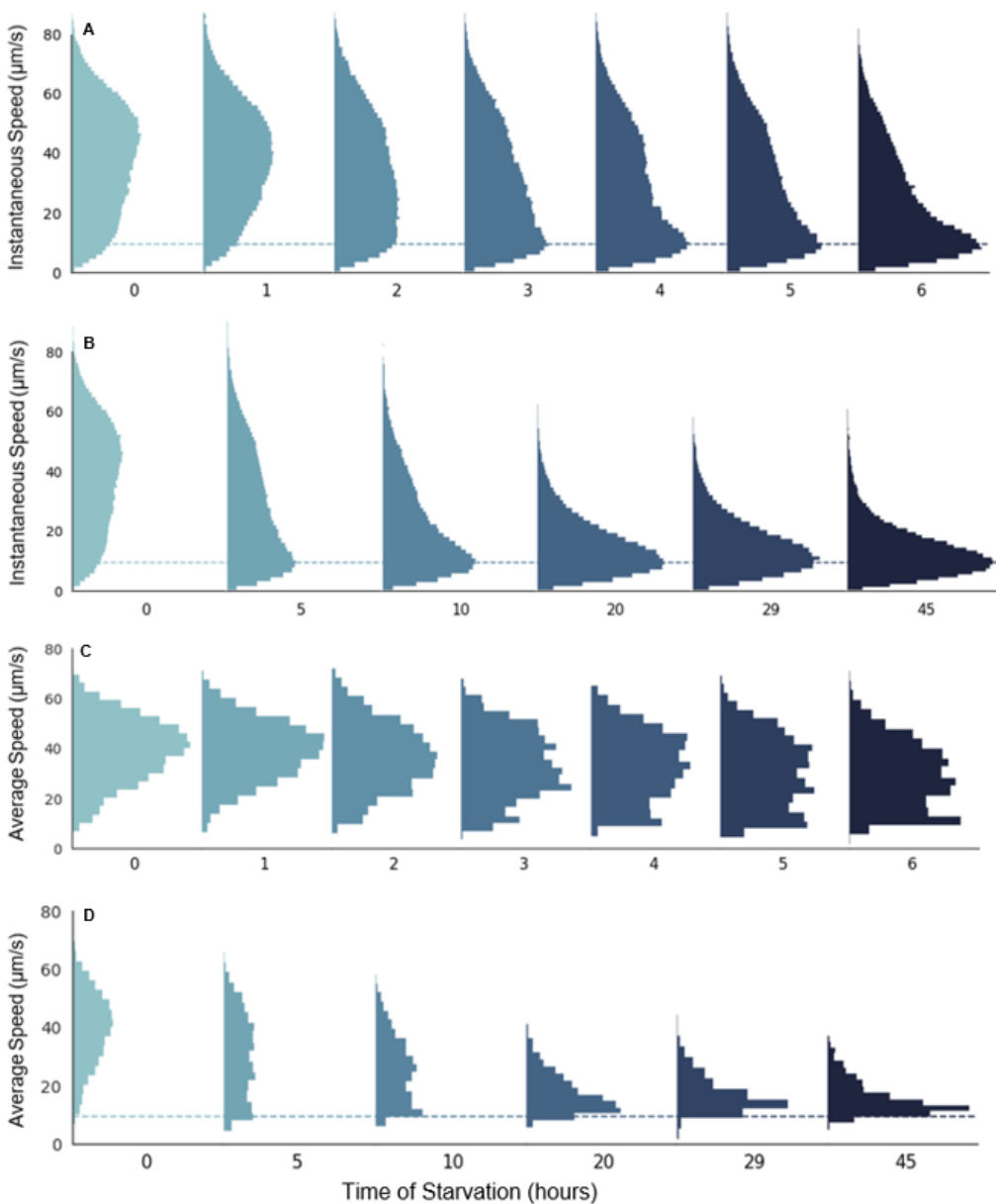
Figure S8: **Under starvation conditions, the instantaneous and average speed distributions of *B. bacteriovorus* shift across time. [run 2].** We follow a similar convention to figure 1 in the main text. The only relevant difference is the number of data points contributing to each histogram. For (A) and (B), the number of instantaneous speed observations ranges from 93,196-172,376; for (C) and (D), the number of average speed observations ranges from 1,327-3,277.
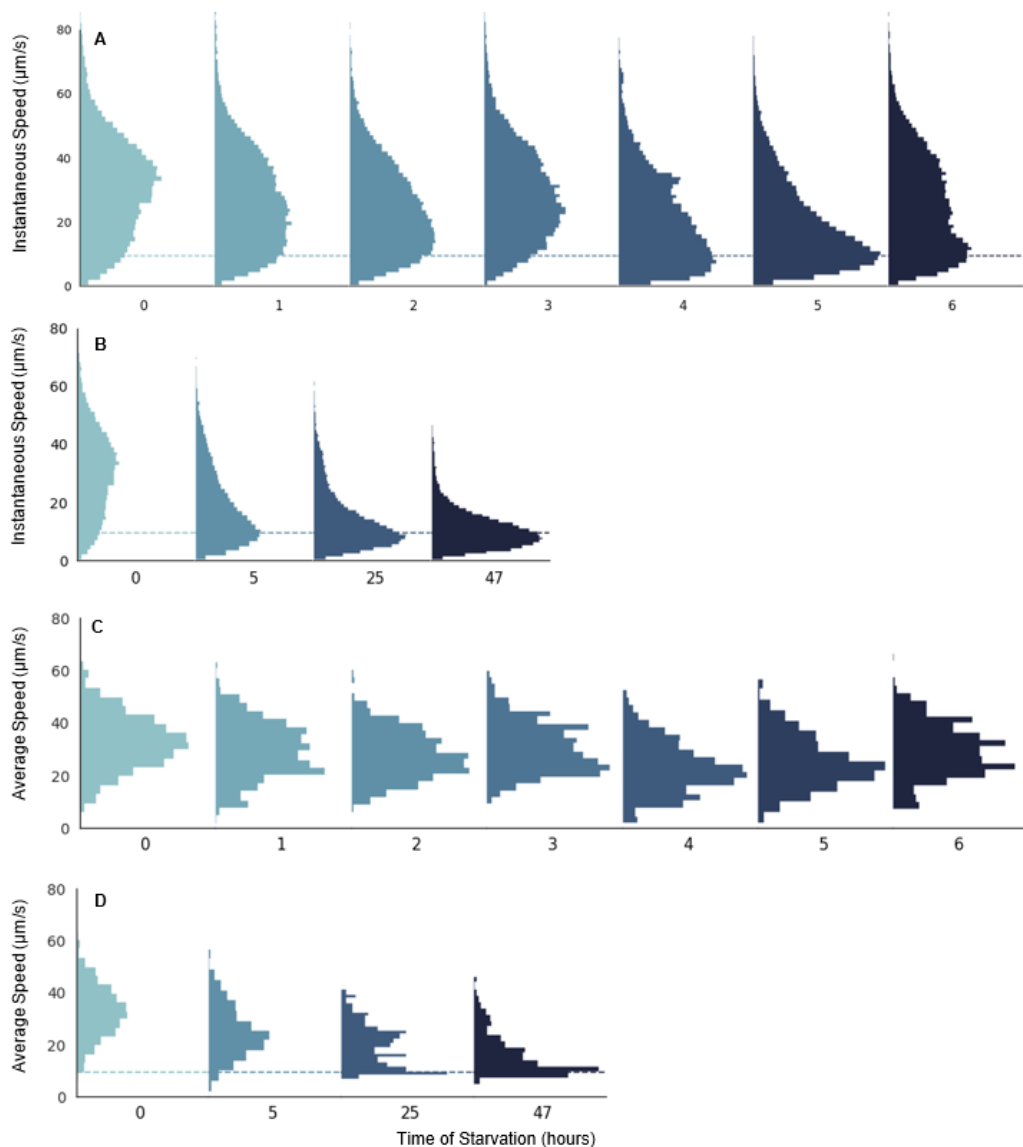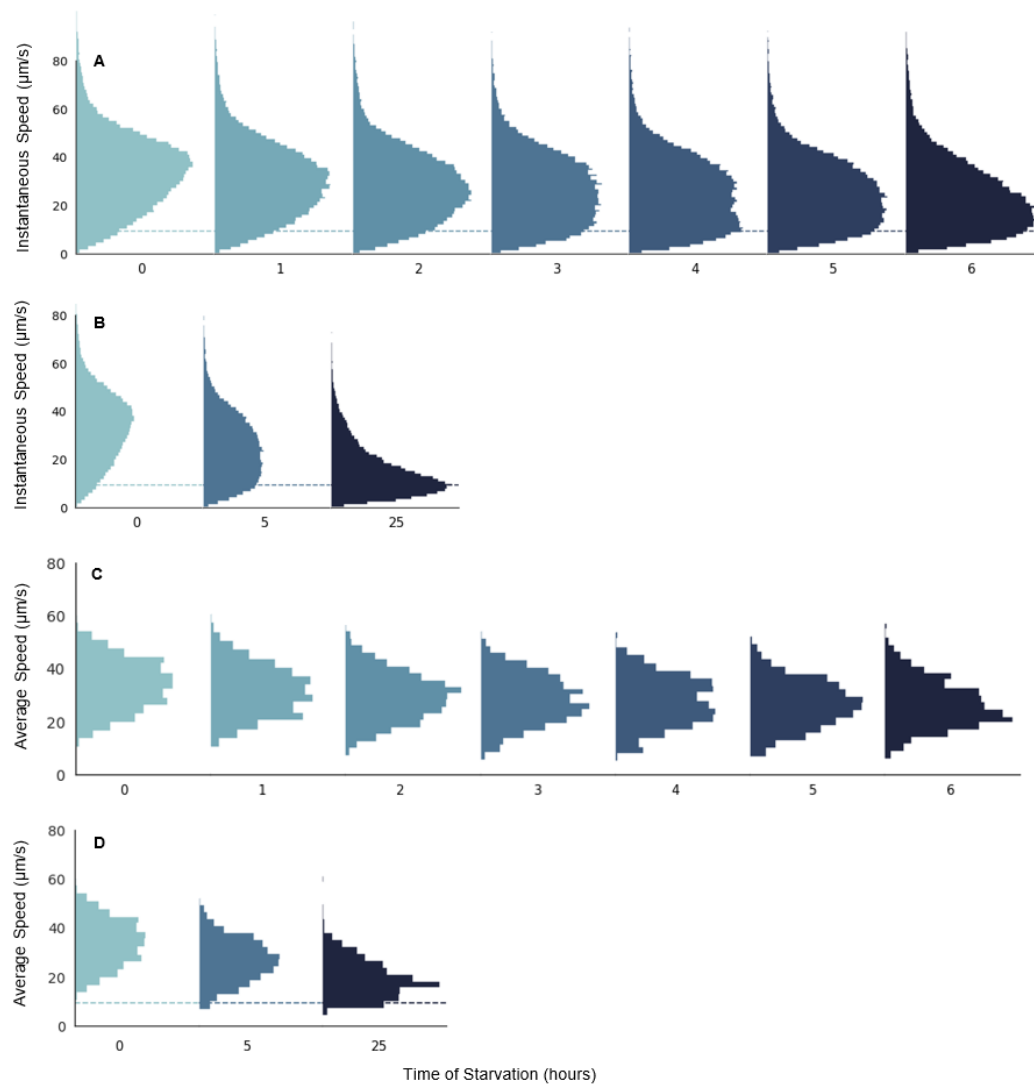
Figure S9: **Under starvation conditions, the instantaneous and average speed distributions of *B. bacteriovorus* shift across time [run 3].** We follow a similar convention to figure 1 in the main text. The only relevant difference is the number of data points contributing to each histogram. For (A) and (B), the number of instantaneous speed observations ranges from 25,959-60,393; for (C) and (D), the number of average speed observations ranges from 247-982.

Figure S10: **Under starvation conditions, the instantaneous and average speed distributions of _B. bacteriovorus_ shift across time [run 4].** We follow a similar convention to figure 1 in the main text. The only relevant difference is the number of data points contributing to each histogram. For (A) and (B), the number of instantaneous speed observations ranges from 49,264-107,299; for (C) and (D), the number of average speed observations ranges from 500-2,065.
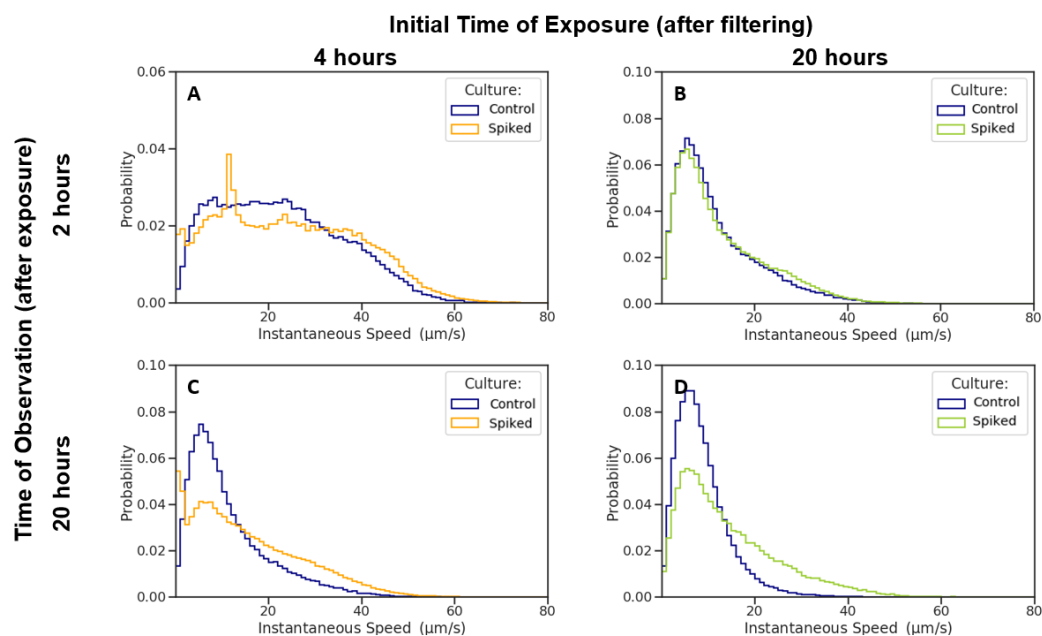
Figure S11: **After addition of LB, *B. bacteriovorus* begins to swim more often even after long starvation times [run 2].** We follow a similar convention to figure 2. The number of instantaneous speed observations ranges from 65,795-110,082 for (A), 84,361-174,041 for (B), 80,625-95,618 for (C), and 141,373-96,026 for (D). Distributions were constructed from 100 evenly spaced bins over the range of instantaneous speed measurements.
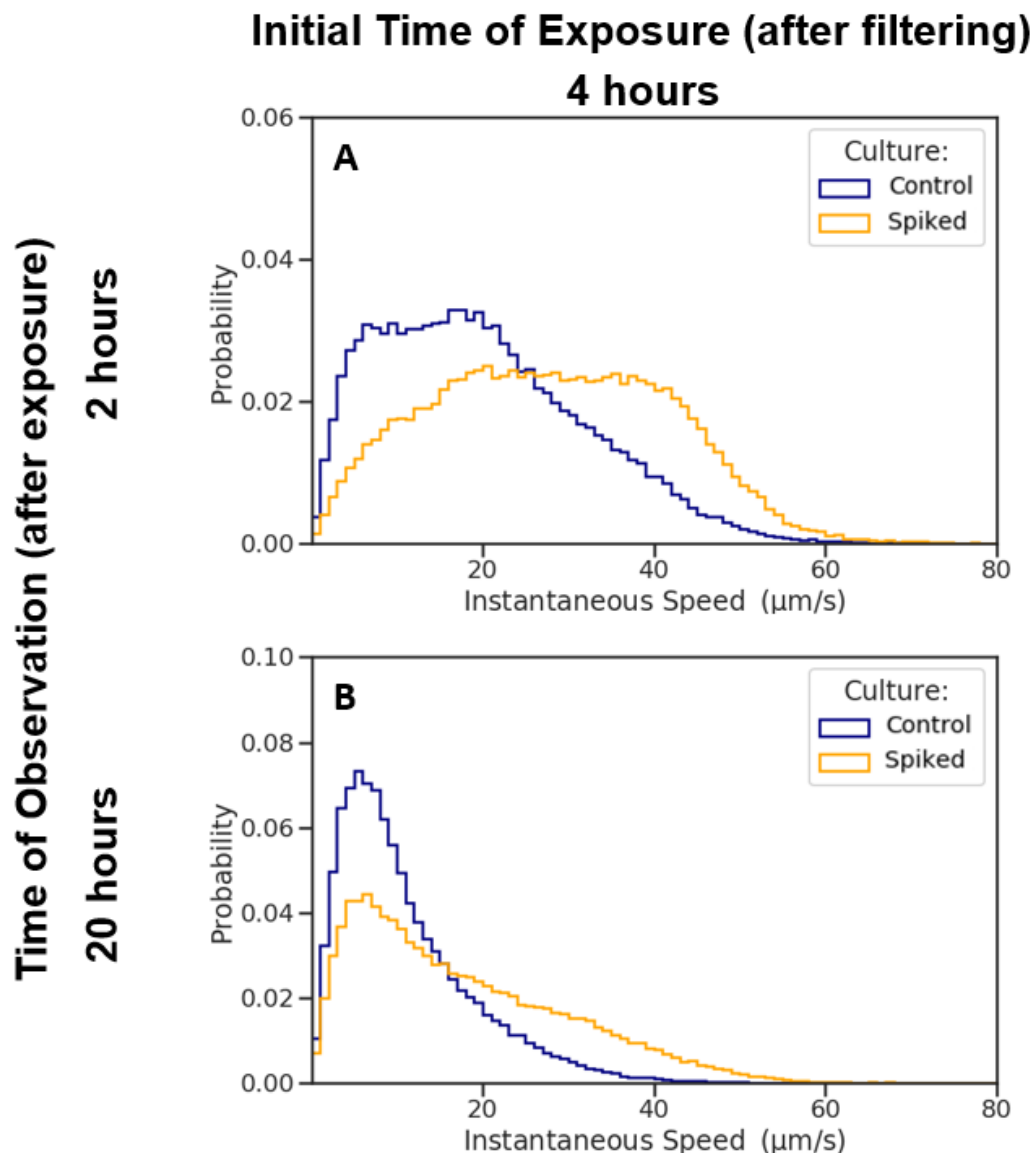
## Initial Time of Exposure (after filtering)



Figure S12: **After addition of LB, *B. bacteriovorus* begins to swim more frequently even after long starvation times [run 3].** We follow a similar convention to figure 2 The number of instantaneous speed observations ranges from 71,290-64,100 for (A) and 68,325-126,841 for (B). Distributions were constructed from 100 evenly spaced bins over the range of instantaneous speed measurements.
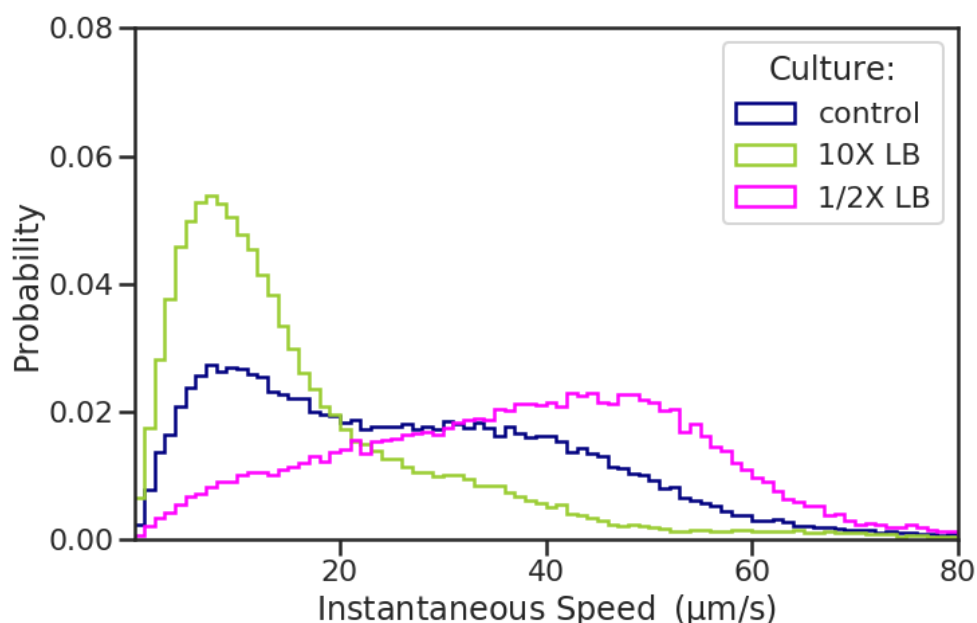
Figure S13: **The speed distributions of spiking experiment is concentration dependent.** A culture starved for four hours and then split into three cultures. One culture remained starving (blue) while the other two were spiked with 10X LB (green) or 1/2X LB concentration (magenta). The culture spiked with the higher concentration resulted in an increase in the apparent diffusive peak whereas the 1/2X culture exhibited an increase in the higher mode peak. This is likely due to an increase in the osmolarity of the solution with the greater concentration of LB. The number of instantaneous speed observations ranges from 49,390-96,644. The data were divided into 100 evenly spaced intervals.
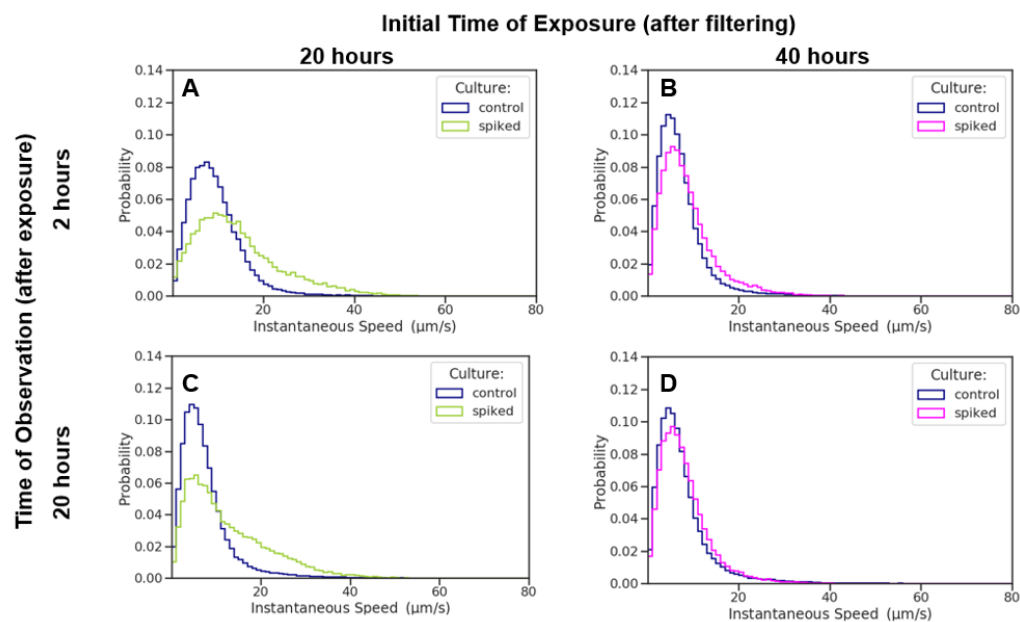
**Initial Time of Exposure (after filtering)**



Figure S14: ***B. bacteriovorus* shows no signs of revival after 40 hours of starvation.** We compare the instantaneous speed distributions of our control, starving *B. bacteriovorus* (blue), to that of cultures spiked with LB at Hour 20 (green) and Hour 40 (magenta). Both spiked cultures were observed after 2 hours and 20 hours of exposure. (A) After two hours of exposure, the culture spiked at Hour 20 (green) has faster speeds than the respective control (blue). (B) After two hours of exposure, the culture spiked at Hour 40 has no noticeable change from the control (blue). (C) After 20 hours of exposure, the culture spiked at Hour 20 still has faster instantaneous speeds than the control. (D) After 20 hours of exposure, the culture spiked at Hour 40 has no noticeable change from the control. The number of instantaneous speed observations ranges from 23,472-45,607 for (A), 28,377-79,194 for (B), 46,801-91,407 for (C), and 38,886-84,523 for (D). Distributions were constructed from 100 evenly spaced bins over the range of instantaneous speed measurements.
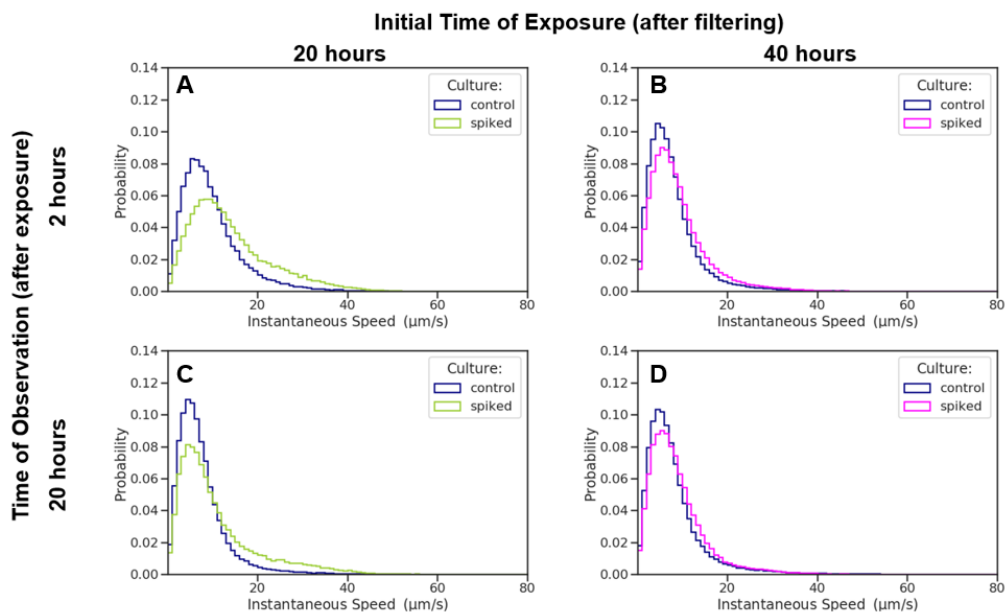
Figure S15: ***B. bacteriovorus* shows no signs of revival after 40 hours of starvation [run 2].** We follow a similar convention to S14. The number of instantaneous speed observations ranges from 36,346-37,567 for (A), 53,562-114,970 for (B), 72,445-110,723 for (C), and 80,017-188,080 for (D). Distributions were constructed from 100 evenly spaced bins over the range of instantaneous speed measurements.

## Sampling statistics for main text figures

Figure 1: The area of each histogram is normalized to unity. For (A) and (B), the number of instantaneous speed observations ranges from 65,795-151,604; for (C) and (D), the number of average speed observations ranges from 621-2,589. Instantaneous speed distributions were constructed from 50 evenly spaced bins over the range of instantaneous speed measurements; average speed distributions were constructed from 30 evenly spaced bins over the range of average speed measurements.

Figure 2: The area of each histogram is normalized to unity. The number of instantaneous speed observations ranges from 39,244-39,862 for (A), 29,943-30,707 for (B), 18,841-20,320 for (C), and 56,115-60,393 for (D). Distributions were constructed from 100 evenly spaced bins over the range of instantaneous speed measurements.

Table S1: **Speeds measured at bounding frames after removal of *n* edge frames.**

| Bounding frames | Number of frames removed from edge | | | | | |
|---|---|---|---|---|---|---|
| | **0** | **1** | **2** | **3** | **4** | **5** |
| $< 30\,\mu\text{m s}^{-1}$ | 4303 (55%) | 3310 (43%) | *2885 (37%)* | 2921 (38%) | 2976 (38%) | 3039 (39%) |
| $> 30\,\mu\text{m s}^{-1}$ | 3464 (45%) | 4457 (57%) | *4882 (63%)* | 4846 (62%) | 4791 (62%) | 4728 (61%) |
| Total | 7767 (100%) | 7767 (100%) | *7767 (100%)* | 7767 (100%) | 7767 (100%) | 7767 (100%) |

Speeds measured at the beginning or end of a trajectory are biased towards lower speeds because bacteria moving into or out of focus are more likely to have a *z*-component to their velocity while motion occurs in the *xy*-plane. To determine the degree of bias, between 0 and 5 *edge frames* were trimmed from the beginning and end of all trajectories and the speeds re-measured for the three bounding frames (at the beginning and end of each trajectory). The number (and percentage) of samples above and below $30\,\mu\text{m s}^{-1}$ are counted after trimming a given number of edge frames. Removing roughly two edge frames (emphasized above) is sufficient to compensate for the slow speed bias at the ends of trajectories; the percentage of slow speed samples settles around 38%.
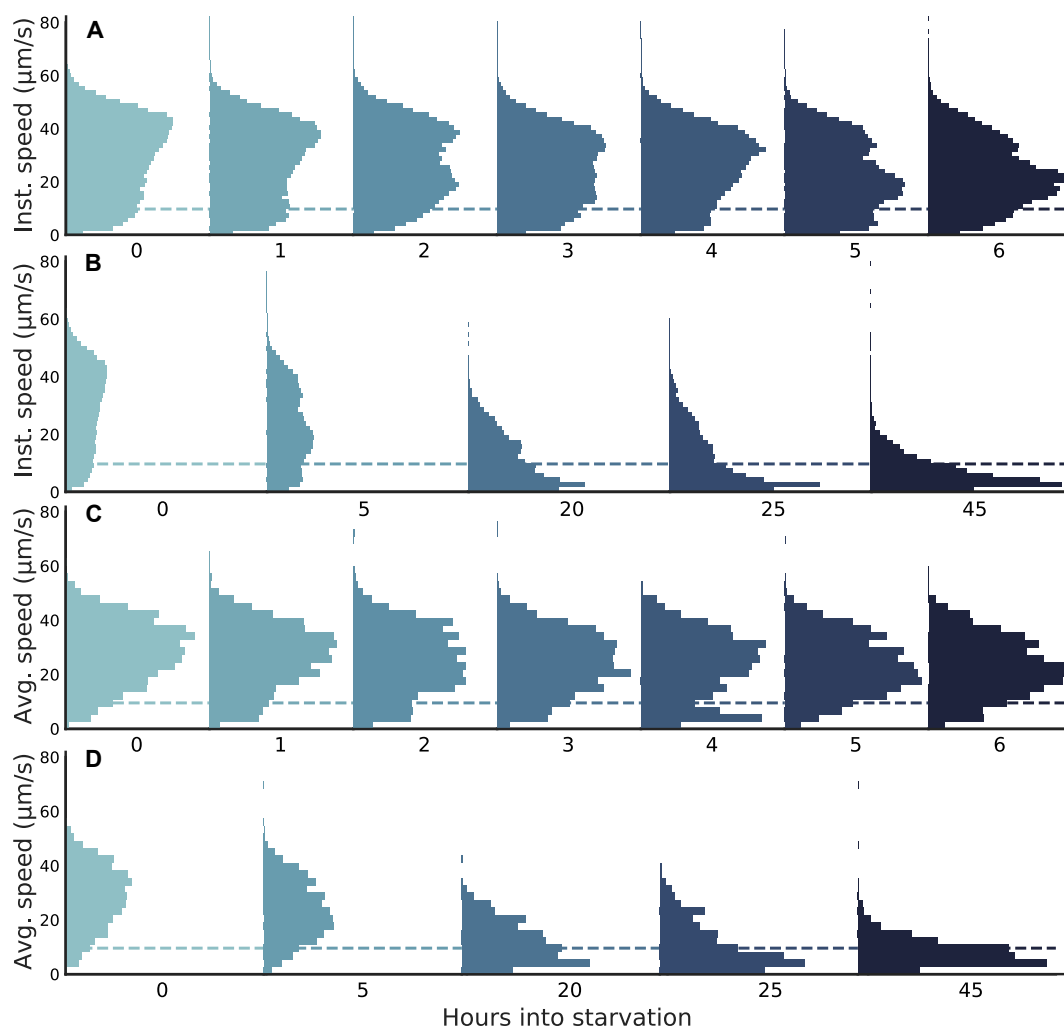
Figure S16: **Recreation of figure 1 with parameter free inference.**

## Comparison to another analysis method

To confirm that our results are independent of the analysis method we performed the same localization and tracking analysis using a different framework. For this secondary analysis method we annotated roughly 1000 images by hand, then trained a neural network (based on MMDetection (1)) to automate the remaining localizations. The mean error between hand annotated localizations and neural net localizations was roughly 4 pixels, as seen in figure S3, which is small considering the average width of a *B. bacteriovorus*' diffraction pattern is around 10 pixels (see figure S3). We linked localizations across frames using TrackPy (2). In order to smooth the linked localizations (*i.e.*, tracks), we used a Gaussian process with a squared exponential kernel (3). The parameters of the kernel were then determined by maximizing the likelihood of the trajectory assuming a Gaussian emission model for the localization error.

Figure S16 shows the results of our inference on the same data as in figure 1. As seen in figure S16 we recover a speed histogram that closely matches that of figure 1. In particular the bimodal behavior is evident in both figures. We note however that the secondary analysis method underestimates the speed in the later experimental hours (> 20 hours of starvation). This is because, in the absence of movement the Gaussian process smoothing averages over the stochastic Brownian motion resulting in a speed distribution close to zero. For this reason, we only use this inference to validate the bimodality of the speed histograms, and we use the window average smoothing method explained in the Methods section for the core of our analysis.

In order to further demonstrate the bimodality of *B. bacteriovorus*, we performed a Gaussian mixture fitting on the results of instantaneous speed, as shown in Table S2. The fitting results for the distributions of instantaneous speed during Hours 0-6 revealed two consistent means, approximately $14\,\mu\mathrm{m\,s^{-1}}$ and $35\,\mu\mathrm{m\,s^{-1}}$. Furthermore, the weight of the faster speed increased from Hour 0 to Hour 6. After a 20-hour period of starvation, our fitting results indicated that the mean value of $35\,\mu\mathrm{m\,s^{-1}}$ was no longer present.

Table S2: **Instantaneous speed distributions at different Hours fitted by Gaussian mixtures.**

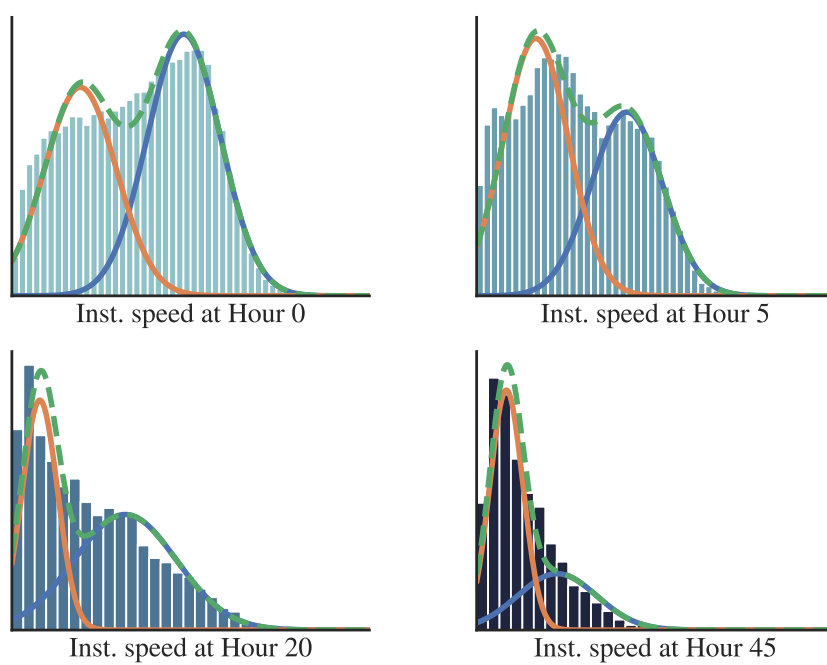| Hour | 0 | 1 | 2 | 3 | 4 |
|---|---|---|---|---|---|
| Weights | 0.440, 0.560 | 0.427, 0.573 | 0.508, 0.492 | 0.479, 0.521 | 0.437, 0.563 |
| Means ($\mu\mathrm{ms^{-1}}$) | 15.3, 38.5 | 13.7, 36.5 | 15.7, 37.1 | 13.7, 34.2 | 13.9, 33.9 |
| Variances ($\mu\mathrm{m^2s^{-2}}$) | 65.1, 67.3 | 57.5, 66.1 | 59.0, 62.1 | 52.4, 63.2 | 58.6, 61.5 |
| Hour | 5 | 6 | 20 | 25 | 45 |
| Weights | 0.565, 0.435 | 0.591, 0.409 | 0.408, 0.592 | 0.420, 0.580 | 0.648, 0.352 |
| Means ($\mu\mathrm{ms^{-1}}$) | 13.3, 33.7 | 15.0, 33.4 | 3.91, 15.8 | 3.59, 17.2 | 4.20, 11.3 |
| Variances ($\mu\mathrm{m^2s^{-2}}$) | 53.8, 63.4 | 54.0, 66.9 | 6.17, 51.4 | 4.90, 73.7 | 5.52, 31.0 |

Figure S17: **Gaussian mixture fitting discussed in table S2 visualized at some represent times.** The orange and blue curves represent the probability density functions (PDFs) of the individual Gaussian components, while the green dashed curve represents the overall PDF.

## SUPPORTING REFERENCES

1. MMDetection Contributors. *OpenMMLab Detection Toolbox and Benchmark*. 2018. URL: https://github.com/open-mmlab/mmdetection.

2. Dan Allan et al. *soft-matter/trackpy: Trackpy v0.4.2*. Version v0.4.2. 2019. DOI: 10.5281/zenodo.3492186.

3. Christopher KI Williams and Carl Edward Rasmussen. *Gaussian processes for machine learning*. Vol. 2. 3. MIT press Cambridge, MA, 2006.